HAW HAMBURG

Bachelor Thesis

Fuel Consumption of the 50 Most Used Passenger Aircraft as Function of Flight Distance

Author: Joel Nisa

Supervisor: Prof. Dr.-Ing. Dieter Scholz, MSME
Submitted: 2025-07-11

Faculty of Engineering and Computer Science
Department of Automotive and Aeronautical Engineering

DOI:
https://doi.org/10.15488/xxxxx

URN:
https://nbn-resolving.org/urn:nbn:de:gbv:18302-aero2025-07-11.01
Associated URLs:
https://nbn-resolving.org/html/urn:nbn:de:gbv:18302-aero2025-07-11.01

Any further request may be directed to:
Prof. Dr.-Ing. Dieter Scholz, MSME
E-Mail see: http://www.ProfScholz.de

This work is part of:
Digital Library - Projects & Theses - Prof. Dr. Scholz
http://library.ProfScholz.de

Published by
Aircraft Design and Systems Group (AERO)
Department of Automotive and Aeronautical Engineering
Hamburg University of Applied Science

This report is deposited and archived:
- Deutsche Nationalbiliothek (https://www.dnb.de)
- Repository of Leibniz University Hannover (https://www.repo.uni-hannover.de)
- Internet Archive (https://archive.org)
  Item: https://archive.org/details/TextNisaLopez.pdf

This report has associated published data in Harvard Dataverse:
https://doi.org/10.7910/DVN/6FWVDM

Abstract

Purpose – The estimation of aircraft fuel consumption of passenger aircraft over varying flight distances is essential in flight planning and environmental assessment. The so-called bathtub curve represents fuel consumption per passenger per 100 km versus flight distance but is not discussed much. This could be changed by representing the function with a simplified analytical equation. As an example, the new function is applied for Intermediate Stop Operations (ISO).

Methodology – Necessary for the calculation are only Maximum Take-Off Mass (MTOM), Maximum Zero-Fuel Mass (MZFM), number of seats, average mass of one passenger (including baggage) and the payload-range diagram of the aircraft. Using these numbers and the Excel table developed by Burzlaff (2017), the fuel consumption was represented as a function of flight distance and five fitted constants (*a, b, c, d, e*) for each of 50 of the most used passenger aircraft. The constants were fitted using Excel's Solver. With an Excel table, the aircraft with the lowest fuel consumption for a given flight distance was determined for normal operation as well as for different ISO strategies.

Findings – Fuel consumption represented with the bathtub curve was determined and successfully approximated for 50 aircraft, revealing minimum fuel consumption and its flight distance for each aircraft type. The analytical equation showed minimal deviation from the full model. The ISO analysis, applied to the Perth–London route, showed that using a range-optimized aircraft for two legs can reduce fuel per passenger compared to a single-leg flight by 7.5%.

Research Limitations – The calculation of aircraft fuel consumption is limited only by available data. Mostly, sufficient input data is available or can be estimated.

Practical Implications – Now, absolute fuel consumption and fuel consumption per passenger and 100 km as a function of flight distance can easily be calculated. Respective solutions are given for 50 passenger aircraft. For a given flight distance, the aircraft with the lowest fuel consumption can be found. This also allows a quick answer for possible savings from ISO.

Social Implications – Passenger aircraft fuel consumption as a function of flight distance can be discussed openly independent of otherwise missing manufacturer's data based on a simple equation.

Originality – While the bathtub curve itself is not new, this work expands its use by proposing an analytical approximate equation for fast calculations and provides results for 50 passenger aircraft.

HAW HAMBURG

DEPARTMENT OF AUTOMOTIVE AND AERONAUTICAL ENGINEERING

Fuel Consumption of the 50 Most Used Passenger Aircraft as a Function of Flight Distance

Task for a *Bachelor Thesis*

Background

Aircraft fuel consumption depends strongly on stage length, as a considerable amount of fuel is required for take-off and climb. This fuel expenditure is not fully recuperated during descent and landing. Moreover, flying extremely long-range routes necessitates a reduced payload to accommodate the additional fuel required. This relationship between fuel consumption and stage length is visualized with the bathtub curve and can be approximated using a simple equation. As an example, the bathtub curve is applied to fuel calculations in Intermediate Stop Operation (ISO). ISO has the potential to reduce per-passenger fuel consumption. Instead of conducting an ultra-long-haul flight in one leg, the journey is divided into two flight legs, each covering approximately half the full flight distance. On the two shorter flights, the aircraft can avoid high per-passenger fuel consumption at reduced payload. It is also possible to select a more efficient aircraft with shorter range. However, the approach faces practical difficulties such as increased operational complexity, additional airport fees and emissions, as well as extended overall travel time.

Task

The task of this Bachelor Thesis is to analyze aircraft fuel consumption using the bathtub curve and to apply it to ISO as an example. The subtasks are:

- Present the state of the art with a small literature review (bathtub curve, analytical equation, ISO).
- Calculate the bathtub curve using our Excel Table with data from our Aircraft Database among input data also from other sources.
- Extend the calculation to find the analytical (approximate) simple equation.
- Apply the above calculations to the 50 most used passenger aircraft.
- Analyze the parameters of the approximate version of the bathtub curve.
- Extend the calculation to obtain the absolute fuel consumption for a given range.
- Assess the potential for ISO with the bathtub curve using the same long-range aircraft and alternatively using an aircraft better suited for the shorter ISO legs.
- Evaluate the practical implications of ISO.

The report has to be written in English based on international standards on report writing.

Table of Contents

List of Figures

List of Tables

List of Symbols

B	Breguet Factor
c	Thrust Specific Fuel Consumption (TSFC)
c'	Power Specific Fuel Consumption (PSFC)
D	drag
E	glide ratio ($E = L/D$)
g	gravitational acceleration
L	lift
m	mass
m_{pax}	mass of one passenger
M_{cruise}	cruise Mach number
M_{ff}	fuel fraction
n_{pax}	number of passengers
n_{seat}	number of seats
P_D	drag power
P_S	shaft power
Q	fuel mass flow
R	range
t	time
T	thrust
V	cruise speed (expressed as true airspeed)
W	weight ($W = m\ g$)
η_P	propeller efficiency

List of Abbreviations

ISO	Intermediate Stop Operation
LTO	Landing and Take-off
MFW	Maximum Fuel Weight
MPL	Maximum Payload
MSE	Mean Squared Error
MTOW	Maximum Take-Off Weight
MZFW	Maximum Zero Fuel Weight
OEW	Operational Empty Weight
PL	Payload
PLF	Passenger Load Factor
SFC	Specific Fuel Consumption

List of Definitions

bathtub curve
"Visualization of fuel consumption per passenger and 100 km flight distance over the flown distance." (Burzlaff 20217)

flight leg
"A [flight] leg can also refer to an entire flight. Since airlines make multiple flights a day with the same aircraft, each flight can be identified as a leg." (Paramount 2025)

leg
"Part of a flight pattern that is between two stops, positions, or changes in direction." (Crocker 2005)

Maximum Take-off Weight (MTOW)
"The maximum weight authorized at take-off brake release." (Torenbeek 1976)

Maximum Zero Fuel Weight (MZFW)
"The maximum weight of an aircraft less the weight of the Total Fuel Load." (Torenbeek 1976)

Maximum Fuel Weight (MFW)
"Describes the maximum possible fuel mass, which can be carried by the aircraft. If the MFW is loaded, a payload reduction is necessary." (Burzlaff 2017)

Operational Empty Weight (OEW)
"The weight of the airplane without payload and fuel." (Torenbeek 1976)

range
"The distance an aircraft can travel under given conditions without refueling." (AGARD 1980)

stage length
"The distance a plane flies from takeoff to landing in a single leg." (Paramount 2025)

1 Introduction

1.1 Motivation

As fuel prices rise and environmental regulations tighten, airlines are pressured to optimize fuel use. The bathtub curve offers a visual and analytical way to understand and minimize fuel consumption across flight distances. However, the full calculation can be complex and data-intensive. Furthermore, ISO where a long route is split into two shorter legs has shown potential for reducing overall fuel burn. This thesis explores how to make the bathtub curve more accessible and use it to support strategic decisions such as ISO implementation.

1.2 Title Terminology

Title:
Fuel Consumption of the 50 Most Used Passenger Aircraft as Function of Flight Distance.

fuel
"A substance requiring oxidation for the release of its energy." (AGARD 1980)

consumption
"The process of using up fuel or other resources." (Crocker 2005)

fuel consumption
"The rate at which an engine uses fuel, expressed in units such as miles per gallon or liters per kilometer." (Collins English Dictionary 2025)

passenger
"A person who travels in an aircraft, car, train, etc., and has no part in the operation of it." (Crocker 2005)

aircraft
"A vehicle designed to travel through the air dependent on lift support other than reactions of the air against the Earth's surface." (AGARD 1980)

passenger aircraft
"An aircraft specially designed for carrying people." (Crocker 2005)

flight
"The movement of an object through the atmosphere or through space, sustained by aerodynamic, aerostatic, or reaction forces or by orbital speed; especially, the movement of a man-operated or man-controlled device, such as a rocket, a space probe, a space vehicle, or an aircraft." (AGARD 1980)

distance
"A space between two places or points, or the measurement of such a space." (Crocker 2005)

1.3 Objectives

The objective of this thesis is to analyze and visualize passenger aircraft fuel consumption using the bathtub curve by calculating it for the 50 most commonly used commercial aircraft. This includes deriving the curve through full calculations using the Breguet equation and fuel fractions and then developing a simplified analytical approximation using five fitted parameters to allow for quick and practical estimations. The study also aims to apply these curves to calculate absolute fuel consumption across varying ranges and assess the operational and environmental advantages of Intermediate Stop Operations (ISO).

1.4 Literature

This thesis refers to the project of Burzlaff (2017), where payload-range diagrams were used to determine fuel consumption in a simplified but practical manner. The method demonstrated how key performance data could be derived graphically for different mission profiles.

Furthermore, the work of Kühn (2023) is also taken into account in this thesis. In his project, Kühn focused on evaluating the accuracy of fuel consumption estimations by comparing different aircraft models and validating them against empirical data. His findings support the use of payload-range charts as a reliable source for approximating fuel usage.

1.5 Structure of the Work

The structure of the thesis is as follows:

Chapter 2 provides an overview of the current state of the art, covering fuel consumption modelling methods, usage of the bathtub curve in reliability engineering and aviation, use of other approaches with an analytical simple equation, and the relevance of Intermediate Stop Operations (ISO) in commercial aviation.

Chapter 3 explains the derivation of the bathtub curve, including the mathematical foundation, interpretation, and an analytical approximation method.

Chapter 4 extends the bathtub curve concept to derive total fuel consumption as a function of range.

Chapter 5 assesses the feasibility of Intermediate Stop Operations (ISO), presenting a case study on the Perth–London route and comparing fuel efficiency across different operational models and aircraft types.

Chapter 6 presents a user manual for the Excel tools developed in the thesis, detailing the procedures for calculating the bathtub curve parameters, using simplified models, and selecting suitable aircraft for specific routes.

Appendix A includes the bathtub curves of the most commonly used passenger aircraft.

Appendix B lists the parameters calculated for the analytical version of the bathtub curve for those aircraft.

Appendix C lists the aircraft and the sources where the data for the calculations is extracted from.

2 State of the Art

2.1 Fuel Consumption and Range

Aircraft fuel consumption (kg per 100 km per seat) is significantly influenced by flight distance, primarily due to the high amount of fuel required during the take-off and climb phases of flight. These phases represent a fixed energetic cost that is not fully recovered during descent and landing, especially for short-haul flights. Consequently, as shown in Burzlaff (2017), short flights tend to exhibit higher fuel consumption per passenger-kilometer compared to medium-range flights. The longer the flight the more the initial fuel burn is distributed over the larger distance. The average fuel consumption is reduced accordingly. Finally, at very long flight distances (related to the aircraft's range) fuel consumption increases because payload has to be reduced eventually to zero at the ferry range. The whole phenomenon is graphically represented by the bathtub curve – a U-shaped function.

The curve demonstrates that fuel consumption starts with infinity at flight distance of zero improves with increasing range up to an optimal point, after which it increases again and goes again to infinity at the ferry range.

2.2 Modelling Fuel Consumption

Modelling fuel consumption starts with one representative value for one characteristic flight distance.

Such characteristic fuel consumption values are given in Wikipedia (2025a) in kg/km and in L/100 km per passenger for specified flight distance and for the aircraft capable of flying these typical distances:

- Commuter flights: 300 NM
- Regional flights: 500 NM to 700 NM
- Short-haul flights: 1,000 NM
- Medium-haul flights: 2,000 NM to 3,000 NM
- Long-haul flights: 5,000 NM to 7,000 NM

Kühn (2023) explores various methods for estimating fuel consumption (see Table 2.1).

Table 2.1 Methods for fuel consumption estimation according to Kühn

Method No	Method	Description
1.	**SAR (Specific Air Range)**	Uses the slope of the payload-range diagram. Only takes into account cruise. Good for cruise comparisons. Tends to underestimate fuel consumption. Input of four parameters
2.	**Extended Payload-Range**	Fuel reserves are considered consumed. Input of only three parameters: MTOM, MZFW, and harmonic range. Conservative. Tends to overestimate fuel consumption.
3.	**Bathtub Curve**	Includes all flight phases: LTO, cruise, and weight effect of reserves. Realistic fuel consumption.
4.	**EEA Master Emission**	Includes landing and take-off phase, as well as cruise. Based on BADA. Public data.
5.	**BADA**	Only takes into account cruise. Limited input quality. New BADA requires license.
6.	**Handbook**	Based on handbook equations. Gives a consumption in cruise flight.
7.	**Literature Review**	Compiled from published studies on aircraft fuel consumption; fuel consumption from the Flight Crew Operating Manual (FCOM)
8.	**CO_2 MV**	Based on ICAO / EASA CO_2 metrics. So far almost no data available.

Method 4 (EEA) is the most accurate, while Method 1 underestimates fuel consumption, Method 2 tends to overestimate fuel consumption. Method 3, the bathtub curve, provides realistic coverage by including both LTO and cruise phases with weight effects of reserves. Method 3 is used in this thesis. While Kühn (2023) used the fuel consumption of Method 3 at harmonic range (range at maximum payload), this thesis makes use of fuel consumption as a function of flight distance given by Method 3 (see Chapter 3 for details).

2.3 Bathtub Curves and Analytical Equations

Atmosfair Emissions Calculator

Atmosfair (2008) shows fuel consumption per passenger and 100 km (Figure 2.1). The function does not show the typical bathtub curve because the curve is given for a fully occupied Airbus A340 with 271 seats and does not extend the curve to higher flight distances and reduced payload.

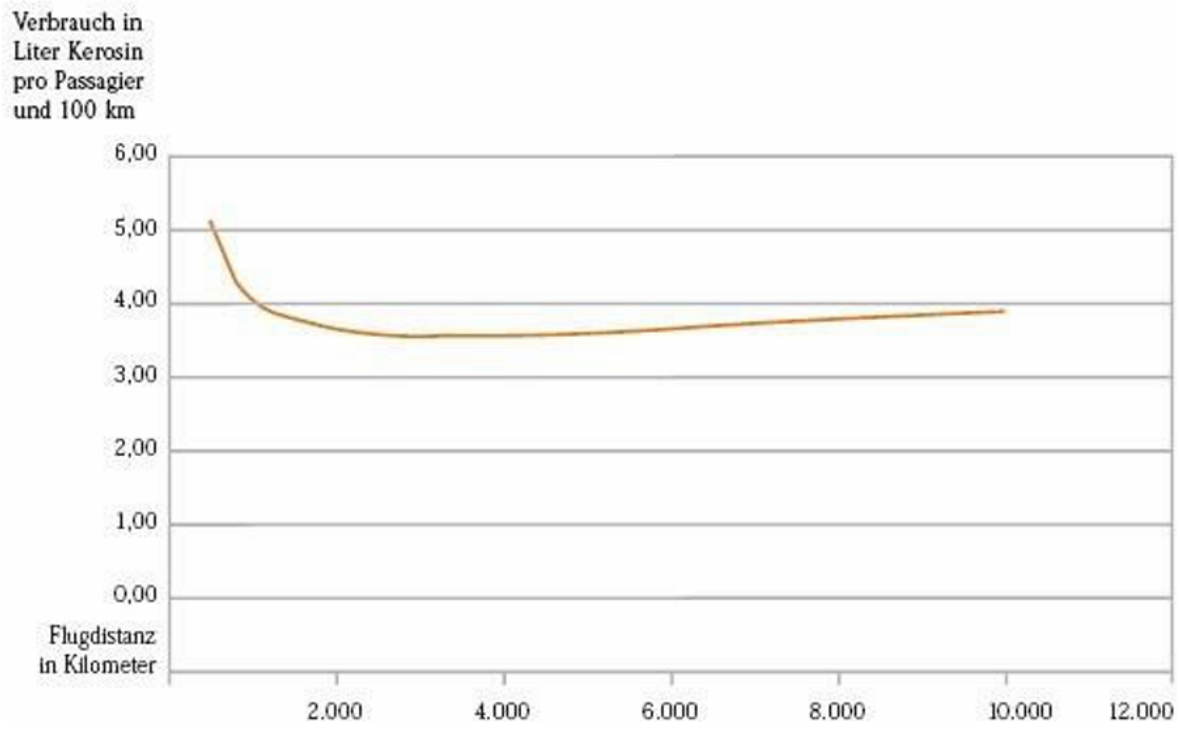

Figure 2.1 Fuel consumption in Liters per passenger and 100 km versus flight distance in km of a fully occupied Airbus A340 with 271 seats as a function of flight distance from Atmosfair (2021) according to the databases "DLR 2000" [1]

The Atmosfair emissions calculator has stored the fuel consumption during the three flight phases (climb, cruise, descent) for the 47 most common aircraft types together with their standard engine originating from the databases "DLR 2000". For each aircraft, these profiles and the corresponding fuel consumption are available for standard distances of 250 km, 500 km, 750 km, 1000 km, 2000 km, 4000 km, 7000 km, and 10000 km (assuming the aircraft can fly that far). To calculate fuel consumption for a given actual distance on a specific flight, the emissions calculator takes the relevant data and interpolates according to the travelled distance. (Atmosfair 2008)

Flight Emissions Calculator MyClimate

The Flight Emissions Calculator from MyClimate (2025) estimates **fuel consumption per aircraft kilometer**, integrating both cruise and non-cruise phases. Fuel consumption is modeled as a function of great circle distance (GCD) and a distance correction (DC) to account for operational inefficiencies such as detours. In addition, a constant is added to each flight to

[1] DLR 2000: Databases were compiled by the German Aerospace Center (DLR) in the year 2000 with emission profiles of civil jets, as part of the study "Measures for the Polluter-Related Reduction of Pollution in Civil Aviation," R&D project 105 06 085, commissioned by the Federal Environment Agency, TÜV Rheinland, DIW, and the Wuppertal Institute for Environment, Climate, and Energy. The databases are stored at the German Federal Environment Agency. The databases are not available to the public.

represent fuel used during the landing, take-off (LTO), and taxi phases. This results in a second-order polynomial approximation for fuel consumption.

$$f(x) + LTO = ax^2 + bx + c \tag{2.1}$$

Where $x = GCD + DC$.

For the "ten most common aircraft types" fuel consumption is retrieved from the EEA Master Emission file for "short-haul (1500 km) and long-haul (>2500 km) flights". "Fuel consumption for distances between 1500 and 2500 km is linearly interpolated." The fuel burn coefficients are derived from a weighted average of aircraft types operated by the largest global and European airlines.

From the description, it remains unclear how the method works. Only ten aircraft and only two flight distance seems to be a rough approach. It is also not clear, if a reduced number of passengers at long flight distances is taken into account.

Analytical Equations Proposed in Scientific Literature

In contrast to MyClimate (2025), Thor (2023) uses a quadratic regression formula (*BF* in Eq. 7 with coefficients in Table 2 in their paper) across seat-size categories for **absolute fuel consumption**.

$$BF = a_0 + a_1 d + a_2 d^2 \tag{2.2}$$

The authors claim high accuracy ($R^2 > 0.99$) of this approach. The method does not take the individual fuel burn characteristics of each aircraft type into account. It is not differentiated between new and old aircraft. Fuel burn per range could be calculated. But the method does not allow to calculate fuel burn per range and seat, because the maximum number of seats as a function of range is not given. This function cannot be given, because the range of individual aircraft types is not accounted for. As such the approach also does not allow to calculate a typical bathtub curve.

Egelhofer (2008) gives an alternative equation (*y* in Eq. 4.1 in the paper) to calculate **relative fuel consumption** per flown kilometer.

$$y = ax + b + \frac{c}{x} \tag{2.3}$$

The calculation is based on optimized mission profiles for each distance, assuming an average load factor. Parameters *a, b*, and *c* are selected to best fit the curve for stage lengths ranging from 300 to 12,000 km. The authors do not provide a table with the specific parameters required to calculate the fuel consumption of each aircraft. Instead, the equation is designed so that these parameters can be determined to approximate the actual curve, which can then be used to estimate potential savings from two-stage operations – an aspect explored in greater depth in the paper.

Overall, the reviewed equations provide valuable groundwork for understanding and modeling fuel consumption and emissions, capturing important aspects of the problem and highlighting the significance of operational phases, aircraft characteristics, and distance effects. However, these methods show notable limitations: simplified assumptions, restricted aircraft or distance ranges, insufficient consideration of passenger load variations, and incomplete data for curve derivation. While these works have paved the way there is a need for a more comprehensive, and accurate approach.

2.4 Intermediate Stop Operation (ISO)

"The goal of intermediate stop operations (ISO, also referred to as staging or multi-step operations) is to increase fuel efficiency by shortening the stage length of a mission by performing one or more intermediate stops for refuelling. Shorter stage lengths allow to reduce the amount of fuel that is needed to carry the required fuel on the respective mission, which reduces the aircraft mass. As a result, kerosene can be saved compared to the non-stop flight." (Zengerling 2022)

Wikipedia (2025b) quotes Filippone (2012) with

> *For long-haul flights, the airplane needs to carry additional fuel, leading to higher fuel consumption. Above a certain distance it becomes more fuel-efficient to make a halfway stop to refuel, despite the energy losses in descent and climb. For example, a Boeing 777-300 reaches that point at 3,000 nautical miles (5,600 km). It is more fuel-efficient to make a non-stop flight at less than this distance and to make a stop when covering a greater total distance.*

and presents a graph of the Boeing 777-200 which shows increasing fuel consumption per flight distance beyond 3000 NM (Figure 2.2), which is not in agreement with my own calculation (Figure 2.3).

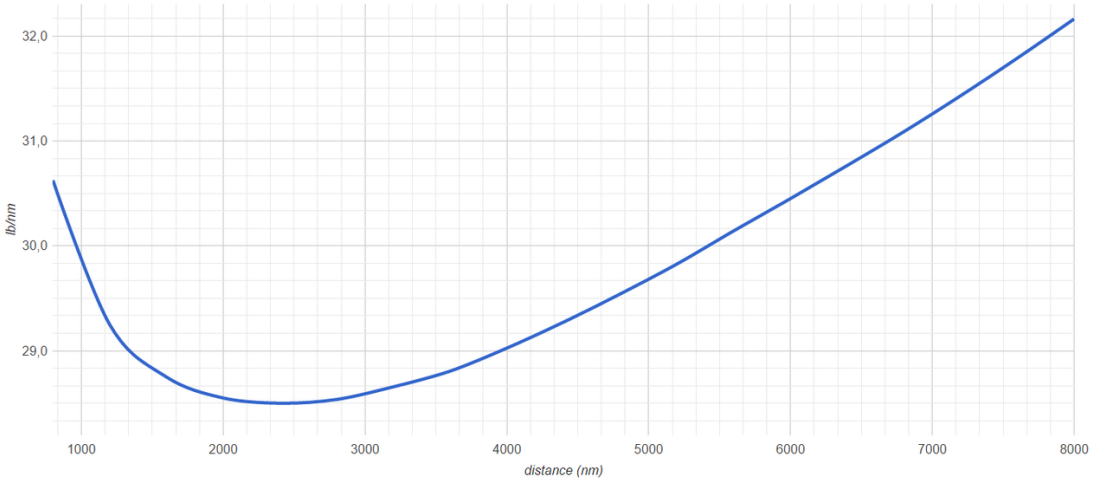

Figure 2.2 Fuel consumption of a Boeing 777-200 per distance in lb/nm. (Wikipedia 2025)

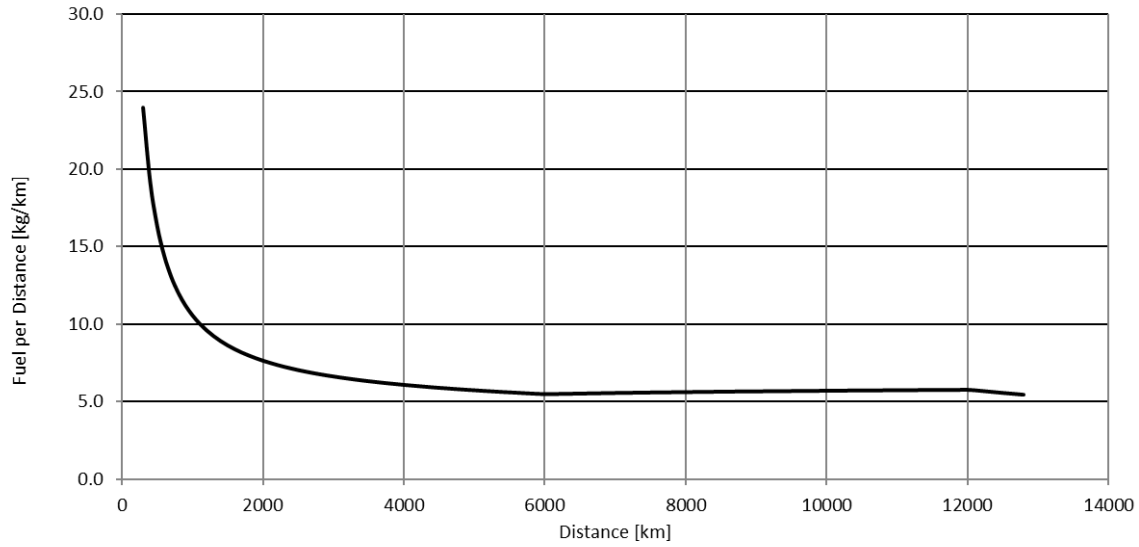

Figure 2.3 Fuel consumption of a Boeing 777-200 per distance in kg/km calculated with the Excel table from Burzlaff (2017b)

There seems to be much disagreement about the characteristics of aircraft fuel consumption. As such it is also not easy to determine if Intermediate Stop Operation (ISO) can reduce fuel consumption or not. Let's look at the big picture.

In the context of increasing operational pressures on legacy airlines due to rising fuel costs, geopolitical instability, and intensified competition from low-cost and Middle Eastern carriers, the aviation sector is exploring alternative strategies to improve efficiency and maintain profitability. Fuel continues to represent a significant portion of airlines' operational expenses – around 35% – despite advancements in aircraft technology and fuel management (Hartjes 2015). As a result, airlines are investigating methods to reduce fuel consumption, including the concept of Intermediate Stop Operations (ISO).

ISO involves dividing a long-haul flight into two or more shorter stages, incorporating landings. This operational strategy can reduce total fuel consumption by limiting the amount of fuel that

needs to be carried from the departure airport, thereby minimizing the transport loss associated with carrying fuel to burn fuel (Linke 2016).

Previous studies and recent case simulations confirm that ISO can yield fuel savings of 5% to 25%, depending on the route and aircraft type (Hartjes, 2015). These savings emerge from more efficient cruise segments and lower take-off weights. However, ISO introduces additional operational costs, including increased landing fees, longer total mission times, altered crew scheduling, and more complex maintenance requirements. To assess whether ISO leads to overall cost savings – not just fuel reduction – Hartjes (2015) developed a software tool incorporating aircraft performance models, cost parameters (crew, maintenance, and fuel prices), and route optimization. Their analysis of various origin-destination pairs revealed that the economic viability of ISO is highly route-dependent, influenced by factors such as local fuel prices, prevailing winds, and required crew configurations.

From an environmental perspective, ISO also shows mixed results. Linke (2016) assessed the climate impact of ISO using a combined modeling approach that included traffic simulation, emissions calculation, and climate response modeling. Their findings indicate that while ISO can reduce global average fuel burn by approximately 5%, the climate impact does not necessarily decrease, they suggest that ISO – when implemented with current wide-body aircraft – may lead to increased warming effects due to higher emissions of nitrogen oxides (NO_x) and water vapor at high cruise altitudes, which outweigh the cooling effects from reduced CO_2 and contrail formation.

According to Egelhofer (2008), as the number of landings and take-offs would be increased, pollutants emitted at low altitudes would also increase beneath the atmospheric mixing height. This phenomenon would compromise local air quality.

Furthermore, the potential benefits would only affect a small fraction of the actual air traffic. Considering 2% fuel savings, the routes worth for two-stage operation would be longer than 7,200 km. Such flights represent only 2.7% of all flights by aircraft greater than 100 seats or 27% of the available seat-kilometers. Multiplying this percentage by the fuel savings, only half a percent of fuel savings is achieved Egelhofer (2008).

3 Bathtub Curve

3.1 Theoretical Foundation

There are many existing ways to estimate the fuel consumption of an aircraft, as it is analysed in Marius Kühn's Project *Fuel Consumption of the 50 Most Used Passenger Aircraft* (Kühn 2023). In this project we will use the bathtub curve, as it takes into account not only the cruise phase, but also the non-horizontal phases and allows us to estimate the fuel mass using available data from aircraft manufacturers. Moreover, the graphical representation of the bathtub curve helps identify the aircraft's optimal flight distance, which will later assist in analysing the benefits of operating ISO with an aircraft specifically suited for half the original flight distance, rather than using a long-range aircraft.

The bathtub curve represents fuel consumption per 100 km per seat and highlights the area of least consumption. In his 2017 project, Burzlaff developed an Excel tool to calculate an aircraft's fuel consumption for a specific flight distance and generate its bathtub curve using publicly available data. To gain a clearer understanding of the bathtub curve's composition, several mathematical relationships are outlined.

Breguet Range Equation

Fuel mass flow, Q is defined as a change of fuel mass per time.

$$Q = -\frac{dm}{dt} \quad . \tag{3.1}$$

In conventional missions, as in our case (passenger engine powered aircraft), a change in mass only depends on fuel burn, so it can be defined as a function of thrust specific fuel consumption, c, glide ratio, E (lift divided by drag), mass, m and gravitational acceleration, g.

$$Q_{jet} = c\,T = c\,\frac{D}{L}\,W = \frac{c}{E}\,m\,g \tag{3.2}$$

Similar for a propeller powered aircraft, the equation depends on the power specific fuel consumption, PSFC, represented by c', the propeller efficiency, η_P, glide ratio, E, mass, m, gravitational acceleration, g, and cruise speed, V. The derivation shows required shaft power, $P_S = P_D/\eta_P$ at the shaft of the engine for mounting the propeller and drag power, $P_D = D\,V$.

$$Q_{prop} = c' P_S = c'\,\frac{P_D}{\eta_P} = \frac{c'\,D\,V}{\eta_P} = \frac{c'\,m\,g\,V}{\eta_P} \cdot \frac{D}{L} = \frac{c'\,m\,g\,V}{\eta_P\,E} \tag{3.3}$$

We define range with velocity, V, and time, t.

$$R = V \cdot t \tag{3.4}$$

Using (3.1) and (3.4) the change of range, dR can be defined.

$$dR = V\ dt = -\frac{V}{Q}\ dm \tag{3.5}$$

The range, R is calculated through integration of (3.5).

$$R = -\int \frac{V}{Q} dm = -\frac{V\ E}{c\ g}\int_{m_1}^{m_2} \frac{1}{m} dm = \frac{V\ E}{c\ g} \cdot [\ln (m)]_{m_1}^{m_2} \tag{3.6}$$

This leads to the Breguet range equation for jet powered aircraft.

$$R = \frac{V\ E}{c\ g}\ \ln\ \frac{m_1}{m_2} \tag{3.7}$$

Breguet Factor

SFC (specific fuel consumption), represented in (3.7) as c and glide ratio, E are not published by the aircraft manufacturer, so we must apply a different procedure to obtain the fuel mass. MacDonald (2012) demonstrates a procedure, which is using the Breguet Factor and enables the Breguet Range equation to be used with only publicly accessible data. This method is explained in Burzlaff (2017).

We define the Breguet factor.

$$B = \frac{V\ E}{c\ g} \tag{3.8}$$

Introducing this factor in the Breguet equation of range we obtain the following expression.

$$R = B\ \ln\frac{m_1}{m_2} \tag{3.9}$$

A rearrangement of (3.9) leads to a new definition of the Breguet factor for simple cruise flight between an airport of origin and an airport for destination, a distance called R apart.

$$B = B_{cruise} = \frac{R}{\ln\frac{m_1}{m_2}} \tag{3.10}$$

The Breguet factor in (3.10) only takes care of cruise or horizontal flight phases. We start over again and include realistically also fuel consumption in non-horizontal flight phases. The full flight can now be described with the mission fuel fraction, defined as $M_{ff} = \frac{m_2}{m_1}$. It consists of mission segment fuel fractions (a little smaller than 1.0). The mass is defined as the mass at the beginning of a flight phase. More details can be found in Scholz (2015, Section 5).

$$M_{ff} = \frac{m_{shut\ off}}{m_{landing}} \cdot \frac{m_{landing}}{m_{loiter}} \cdot \frac{m_{loiter}}{m_{descend}} \cdot \frac{m_{descend}}{m_{reserve}} \cdot \frac{m_{reserve}}{m_{climb}} \cdot \frac{m_{climb}}{m_{descent}} \cdot \frac{m_{descent}}{m_{cruise}} \cdot \frac{m_{cruise}}{m_{climb}} \cdot \frac{m_{climb}}{m_{take\ off}} \tag{3.11}$$

With a simplified notation, this can be written in the following way.

$$M_{ff} = M_{ff,L} \cdot M_{ff,LOI} \cdot M_{ff,DES} \cdot M_{ff,RES} \cdot M_{ff,CLB} \cdot M_{ff,DES} \cdot M_{ff,CR} \cdot M_{ff,CLB} \cdot M_{ff,TO} \tag{3.12}$$

These fuel fractions are separated into two different groups: horizontal and non-horizontal flight phases. Cruise, reserve and loiter are considered horizontal flight, while take-off, climb, descent, and landing are considered non-horizontal flight phases (in short: landing and take-off, LTO).

$$M_{ff} = M_{ff,CR-RES-LOI} \cdot M_{ff,LTO} \tag{3.13}$$

The horizontal flight phases cover the whole distance flown from origin to (planned) destination, plus the distance to an alternate airport, plus the distance flown during loiter (time in holding). These flight phases can be calculated with the Breguet range equation. In contrast, $M_{ff,LTO}$ stands for non-horizontal flight phases and the fuel used *in addition* to covering the horizontal distance. For mission segment fuel fractions *in addition* means *multiplication*. So, the "real" Breguet factor for the "real" flight distance called $R = d_{CR} + d_{RES} + d_{LOI}$ is

$$B = \frac{R}{\ln\left(M_{ff,LTO}\frac{m_1}{m_2}\right)} \quad . \tag{3.14}$$

Fuel Mass Calculation

We will rearrange the Breguet equation using the Breguet factor to finally calculate the fuel mass needed for the flight including all phases.

$$R = B\ \ln\frac{m_1}{m_2} \tag{3.15}$$

m_1 is the mass prior to take-off and m_2 is the aircraft mass after landing. The difference between m_1 and m_2 can be assumed to be the burned fuel mass m_{fuel}.

$$R = B \cdot \ln \frac{m_2 + m_{fuel}}{m_2} \tag{3.16}$$

Finally, rearranging (3.16) we obtain the fuel mass.

$$m_{fuel}(R) = m_2 \left(e^{\frac{R}{B}} - 1 \right) \tag{3.17}$$

Payload-Range Diagram

From now on, as is common when talking about aircraft characteristic masses, weight and mass will be used indistinctly, meaning in both cases what we consider mass in kg.

The manufacturer published payload-range diagrams can be used to extract the necessary data for the calculation of fuel mass and range.

The performance of an aircraft can be described using the payload-range diagram, as seen in Figure 3.1. This chart shows the relationship between the take-off mass and the range achieved in different conditions. We will pay special attention to points A, B, C and D in the chart.

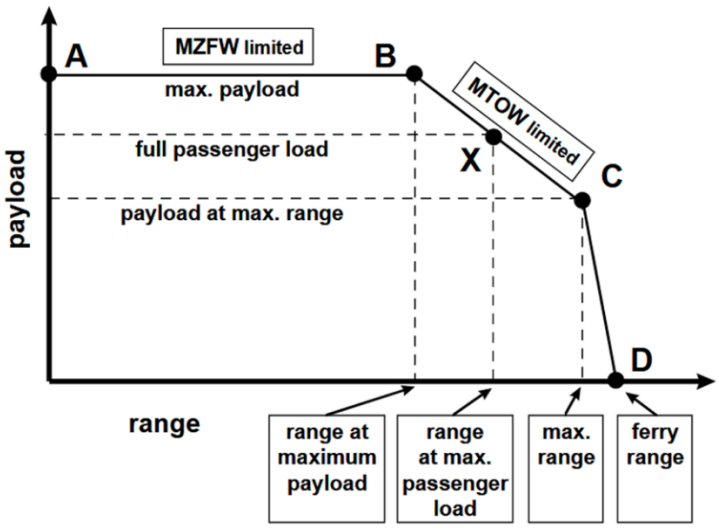

Figure 3.1 Payload-range diagram (Scholz 2015). Note: In Chapter 4 and in the Excel Table, point A is omitted. Accordingly, B is called A, C gets B, and D gets C. A new point D is defined in Chapter 4.

Between points A and B we can see the performance of an aircraft loaded with the maximum payload mass. Point B corresponds to the design point, which means the range achieved with the maximum payload (also called *harmonic range*). At this point we reach MTOW.
Between points B and C we gradually reduce the payload and increase the fuel mass to extend the range. Point C corresponds to an aircraft loaded with full tanks, meaning MFW but still having payload.

Between points C and D the fuel tanks remain fully loaded while payload gets reduced until point D, which corresponds to the ferry range, the maximum distance the aircraft can fly, where the aircraft has full tanks and no payload.

Table 3.1 summarizes the masses at every characteristic point of the payload-range diagram.

Table 3.1 Characteristic points of the payload-range diagram

Point	Range	Take-off weight	Landing weight
B	R_1	*MTOW*	*MZFW*
C	R_2	*MTOW*	*MTOW-MFW*
D	*Ferry Range* $= R_3$	*OEW+MFW*	*OEW*

PL_1 = MPL and OEW = MZFW – PL_1 and MFW = MTOW – (OEW + PL_2). Based on (3.14) we can calculate the Breguet factor for each point of the payload range diagram.

Point B:

$$B_B = \frac{R_1}{\ln\left(M_{ff,LTO}\frac{MTOW}{MZFW}\right)} \tag{3.18}$$

Point C:

$$B_C = \frac{R_2}{\ln\left(M_{ff,LTO}\frac{MTOW}{MTOW - MFW}\right)} \tag{3.19}$$

Point D:

$$B_D = \frac{R_{ferry}}{\ln\left(M_{ff,LTO}\frac{OEW + MFW}{OEW}\right)} \tag{3.20}$$

As payload decreases between B and C, and C and D, a linear interpolation should be made to obtain the correct Breguet factor.

Interpolation between B and C:

$$B_{B-C} = B_B + \frac{B_C - B_B}{R_2 - R_1} \cdot (R - R_1) \tag{3.21}$$

Interpolation between C and D:

$$B_{C-D} = B_C + \frac{B_D - B_C}{R_{ferry} - R_2} \cdot (R - R_2) \tag{3.22}$$

As an example, we will calculate the bathtub curve of the most used airplane in commercial aviation, Boeing 737-800 using the Excel table from Burzlaff (2017). The data used for the calculations is extracted from the Aircraft Dataset (Kühn 2024) and the document "737 Airplane Characteristics for Airport Planning" (Boeing 2024) (see Table 3.3 and its summarized version, Table 3.4).

Data can be extracted from Figure 3.2 (Boeing). It is given in Table 3.2.

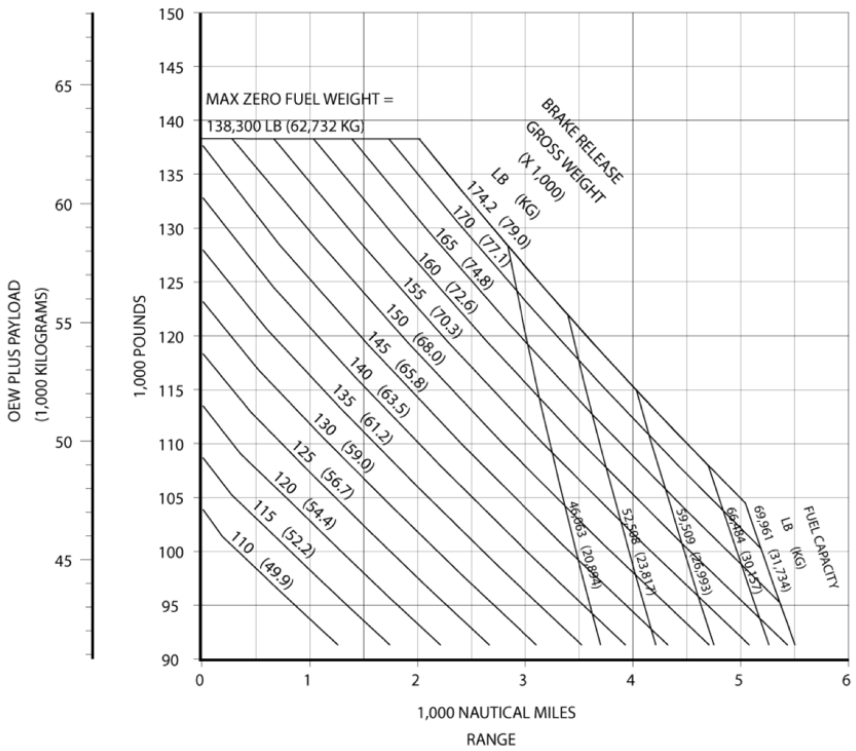

Figure 3.2 Payload-range diagram of Boeing 737-800 from (Boeing 2024)

Table 3.2 Characteristic points of the payload-range chart of B737-800

Required data	Data from payload-range chart
Payload at point B (or 1)	21,184 kg
Range at point B (or 1)	3,750 km
Payload at point C (or 2)	16,716 kg
Range at point C (or 2)	5,298 km
(Ferry) Range at point D (or 3)	6,850 km
Passenger weight	95 kg

Data can be extracted from Table 3.3 (Boeing). It is given in Table 3.4.

Table 3.3 Masses of Boeing 737-800 from (Boeing 2024)

CHARACTERISTICS	UNITS	MODEL 737-800, -800 WITH WINGLETS		
MAX DESIGN - TAXI WEIGHT	POUNDS	156,000	173,000	174,900
	KILOGRAMS	70,760	78,471	79,333
MAX DESIGN - TAKEOFF WEIGHT	POUNDS	155,500	172,500	174,200
	KILOGRAMS	70,534	78,245	79,016
MAX DESIGN - LANDING WEIGHT	POUNDS	144,000	144,000	146,300
	KILOGRAMS	65,317	65,317	66,361
MAX DESIGN - ZERO FUEL WEIGHT	POUNDS	136,000	136,000	138,300
	KILOGRAMS	61,689	61,689	62,732
OPERATING - EMPTY WEIGHT (1)	POUNDS	91,300	91,300	91,300
	KILOGRAMS	41,413	41,413	41,413
MAX STRUCTURAL - PAYLOAD	POUNDS	44,700	44,700	47,000
	KILOGRAMS	20,276	20,276	21,319
SEATING CAPACITY (1)	TWO-CLASS	160	160	160
	ALL-ECONOMY	184	184	184
MAX CARGO VOLUME - LOWER DECK	CUBIC FEET	1555	1555	1555
	CUBIC METERS	44.1	44.1	44.1
USABLE FUEL	US GALLONS	6875	6875	6875
	LITERS	26,022	26,022	26,022
	POUNDS	46,063	46,063	46,063
	KILOGRAMS	20,894	20,894	20,894

Table 3.4 General characteristics of Boeing 737-800 (based on Boeing 2024)

$MPL = PL_1$	21,184 kg	R_1	3,750 km
$MTOW$	79,016 kg	R_2	5,223 km
$MZFW$	62,732 kg	$R_{ferry} = R_3$	6,850 km
PL_2	16,716 kg	M_{cruise}	0.78
m_{pax}	95 kg	n_{seat}	160

The resulting bathtub curve is shown in Figure 3.3.

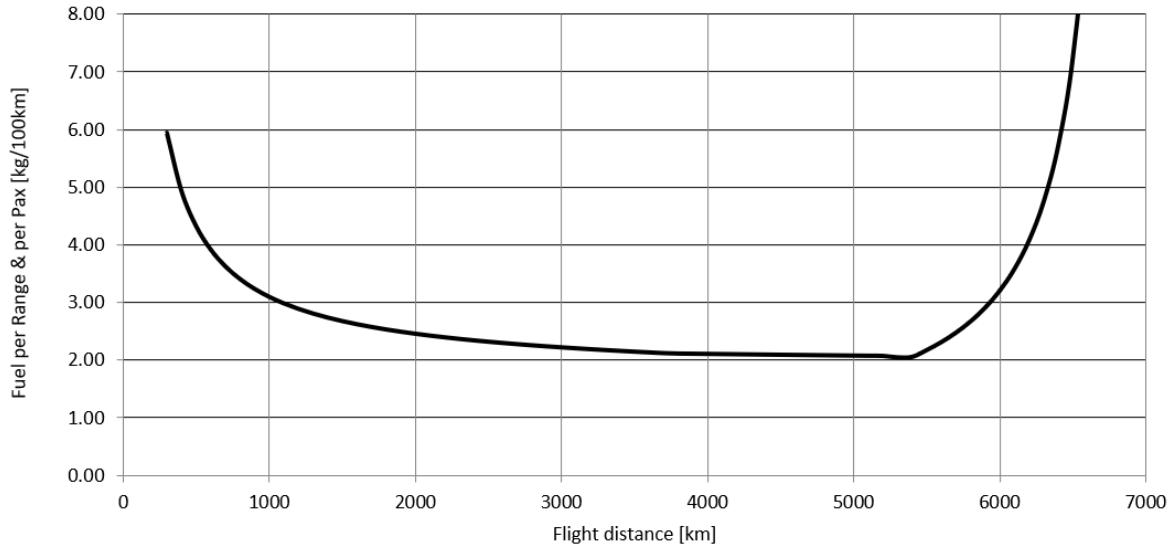

Figure 3.3 Bathtub curve for B737-800 calculated with the Excel Table from (Burzlaff 2017)

As can be seen in Figure 3.3, the fuel consumption per passenger per 100 km increases at both the low and high extremes of the curve, indicating that flying either near the aircraft's ferry range or over very short distances is not optimal. There is a broad region in the graph where fuel consumption remains nearly constant, reaching a minimum in our case at 5,300 km. To maximize fuel efficiency, the aircraft should operate within this flat region.

3.2 Analytical Equation

The fuel mass calculation presented in the previous chapter relies on a fairly complex equation that involves multiple interpolations of the Breguet factor, depending on the segment of the payload-range diagram under consideration. This highlights the need to derive a simplified analytical version of the bathtub curve, one that can easily be used with a pocket calculator.

As shown in Figure 3.3, the bathtub curve exhibits an asymptotic behavior at the beginning, where the fuel consumption per passenger per 100 km tends toward infinity as the flight distance approaches very low values. To approximate this behavior, parameter *a* is included in Equation (3.23), with the independent variable placed in the denominator.

The curve also features a nearly constant central segment, running with a light descending slope to the horizontal axis. This section is represented in (3.23) by the constant *d* and the linear coefficient *e*.

As the curve approaches the ferry range, a similar asymptotic behavior reappears, with fuel consumption per passenger per 100 km increasing sharply. To capture this effect, constants *b* and *c* are added to the analytical approximation.

Thus, (3.23) is obtained, providing an analytical approximation of the bathtub curve.

$$y = \frac{a}{x} + \frac{b}{c - x} + d + ex \tag{3.23}$$

Note the units of the parameters *a*, *b*, *c*, *d* and *e*. Here we work with distances in km and fuel consumption per passenger in kg/(100 km). Accordingly, the units are as given in Table 3.5.

To determine the values of the parameters *a*, *b*, *c*, *d* and *e* in the analytical approximation, an additional table is added to the Excel file from Burzlaff (2017). This table computes, for each flight distance value, the squared error between the simplified bathtub curve and the version obtained through the full calculation. Using Excel's GRG Nonlinear Solver, this error is minimized to identify the optimal parameter values. It is important to note that obtaining a

satisfactory solution requires providing reasonable initial guesses – for example, a value of d between -3 and 3, and assigning to c a value close to the ferry range.

In this way, the parameter values shown in Table 3.5 are obtained for the case of the Boeing 737-800. The mean squared error (MSE) is also calculated using (3.24).

$$MSE = \frac{1}{N}\sum_{i=1}^{N}(f_i - y_i)^2 \tag{3.25}$$

Where N is the number of data points, f_i is the value returned by the model and y_i the actual value for data point i.

Table 3.5 Approximation parameters for Boeing 737-800

a	1,036.46 kg·km/(100 km)
b	2,331.89 kg·km/(100 km)
c	6,843.22 km
d	2.0422 kg/(100 km)
e	$-2.843 \cdot 10^{-4}$ kg/(100 km^2)
MSE	$9.953 \cdot 10^{-3}$

As shown in Figure 3.4, the approximation closely matches the computed bathtub curve overall, although it fails to capture the precise minimum in fuel consumption at 5,300 km.

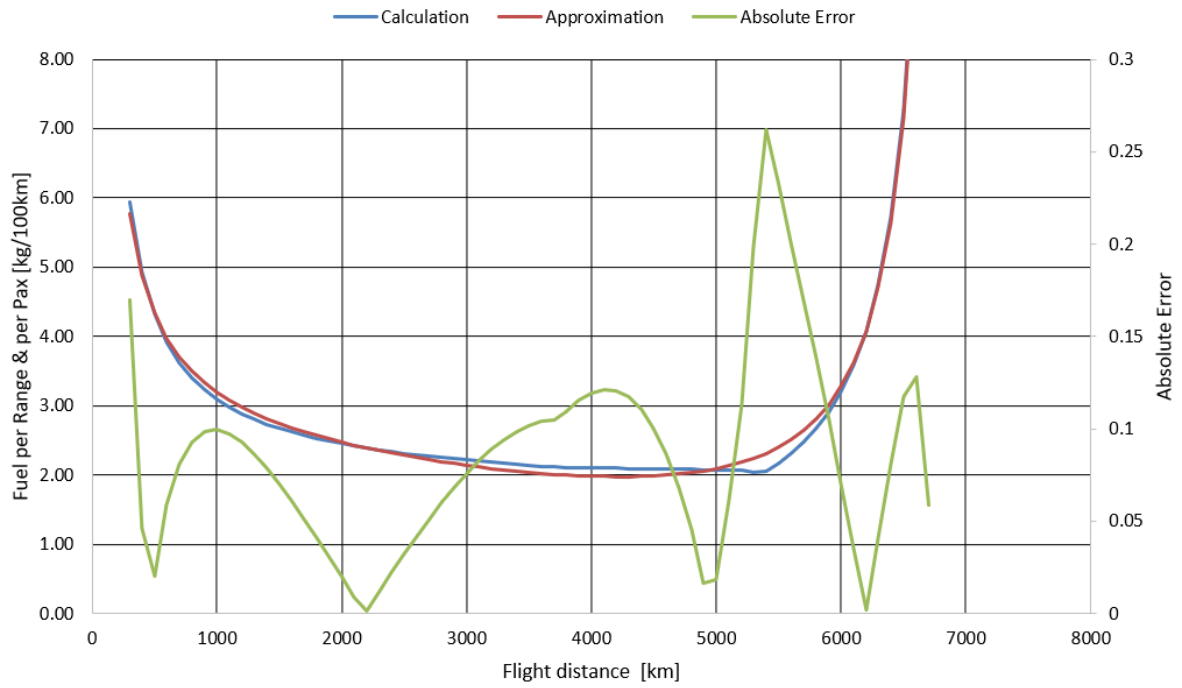

Figure 3.4 Bathtub curve, approximated curve and absolute error for Boeing 737-800

3.3 50 Most Used Aircraft

The bathtub curve calculation is applied to the 50 most commonly used passenger aircraft, using the Excel model developed by Burzlaff (2017), the extended version with the curve approximation, and data extracted from the Excel table by Kühn (2024) and the Aircraft Database by Hirsch (2024). In Appendix C a table contains the names of all the aircraft (in alphabetical order) in one column and the reference where the data can be found in the second column.

To perform these calculations, it is necessary to know the ferry range, which is not included in any of the available datasets. Therefore, it is necessary to source these values from the Manuals for Airport Planning published by the aircraft manufacturers. The reserves assumed in the payload-range diagram must be checked too.

Out of the 50 most commonly used passenger aircraft, the approximation method was successful for all aircraft, yielding a reasonable small margin of error.

It can also be observed that, in some cases, the linear coefficient e is almost negligible – on the order of 10^{-5} or even 10^{-6}– whereas in most cases, it is typically around 10^{-4}.

3.4 Approximate Parameters

The parameters of the analytical equation – a, b, c, d and e – have been successfully calculated for the 50 most commonly used passenger aircraft. Using these data, we will attempt to approximate each of the parameters by leveraging the available values from the aircraft, which have already been used for the complete calculation of the bathtub curve. The final goal is to find a simpler and more time-efficient method to calculate the bathtub curve.

When searching for relationships between the given values of an airplane and the parameters of the approximated bathtub curve, the most evident correlation is with parameter c, which consistently corresponds to the ferry range. This relationship is clearly observed through linear regression, comparing both values for each aircraft (see Figure 3.5).

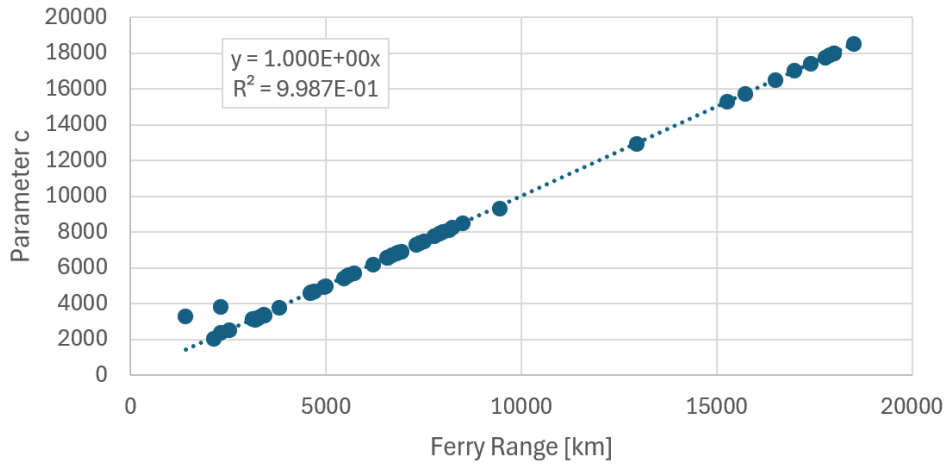

Figure 3.5 *c* versus ferry range of the most used passenger aircraft

The parameter *a* defines the slope of the first arm of the bathtub curve. A relationship has been found between this factor and the ratio of Operational Empty Weight (OEW) to the number of passengers (see Figure 3.6). The heavier an aircraft is, the higher its fuel consumption at lower flight distances, where the consumption per passenger will be significantly higher. In other words, the parameter *a* indicates how much effort the aircraft requires to lift itself.

As the OEW is not one of the parameters required in the excel calculation, the difference between MZFW and maximum payload is used instead.

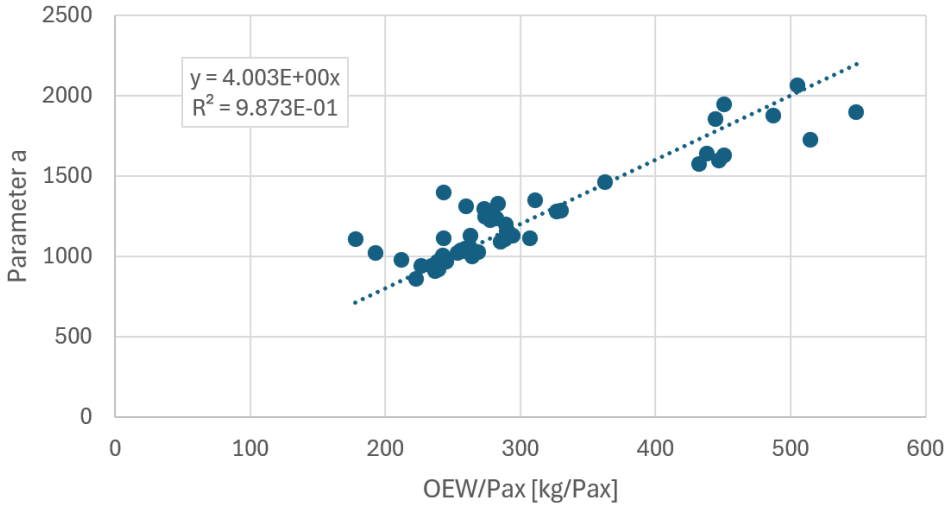

Figure 3.6 *a* versus operational empty weight of the most used passenger aircraft

Since parameter *d* should have units of consumption per distance per passenger, the two methods proposed by Kühn (2023) for calculating consumption are employed to examine whether a clear relationship exists: The SAR-Method and the Extended Payload-Range Method (EPR-Method). These methods are based on simple equations that utilize some of the parameters included in the Excel table prepared for this thesis.

$$c = \frac{1}{\text{SAR n}_{\text{seat}}} \quad \text{where} \quad \frac{1}{SAR} = \frac{MPL - PL_2}{R_2 - R_1} \tag{3.25}$$

$$c = \frac{MTOW - MZFW}{R_1 \, n_{seat}} \tag{3.26}$$

As can be seen in Figures 3.7 and 3.8, there is no clear relationship.

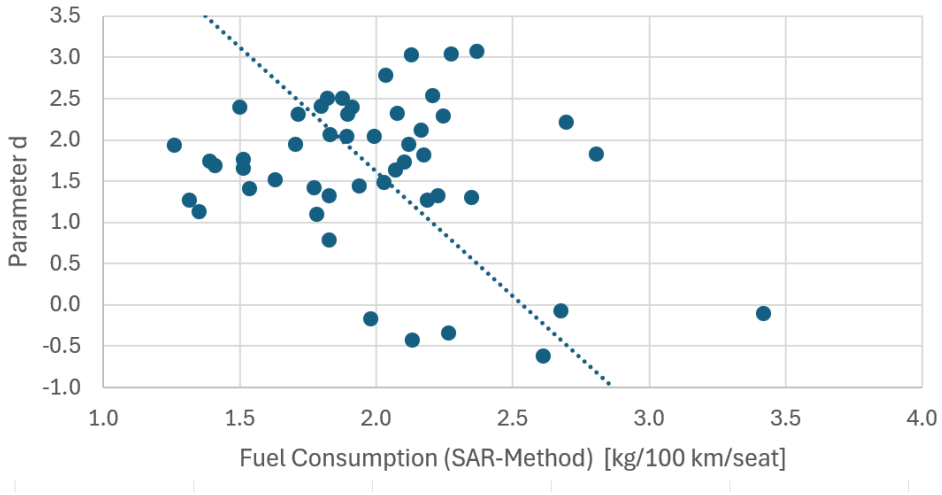

Figure 3.7 *d* versus consumption of the most used passenger aircraft (Method 1)

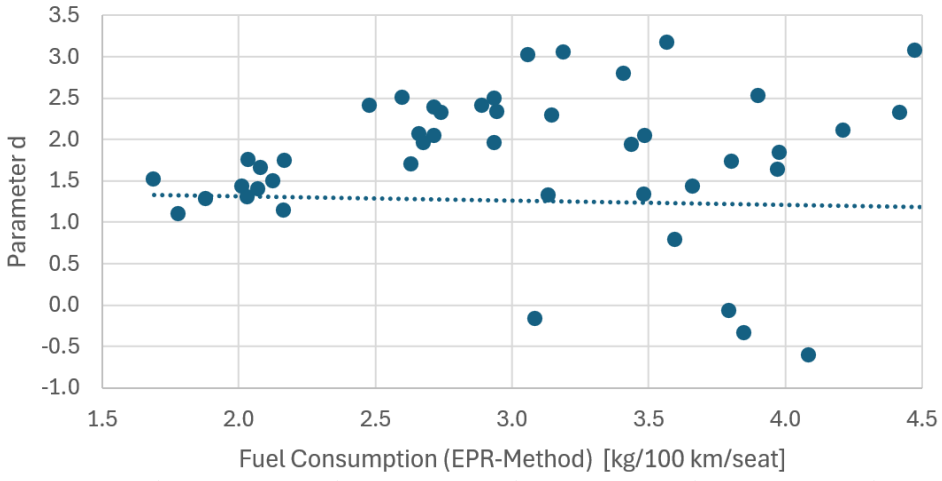

Figure 3.8 *d* versus consumption of the most used passenger aircraft (Method 2)

However, a relationship was found based on this parameter: (MTOW minus MPL) divided by the number of seats. This ratio is related to parameters *b* and *d* (see Figure 3.9 and Figure 3.10). (MTOW minus MPL) is equal to (OWE plus the fuel mass at harmonic range). The ratio is the mass burden per seat.

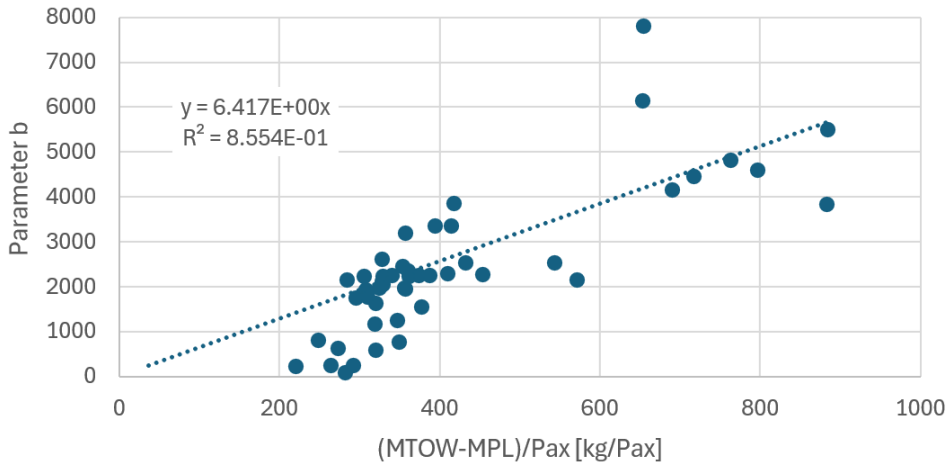

Figure 3.9 *b* versus (MTOW-MPL)/Pax of the most used passenger aircraft

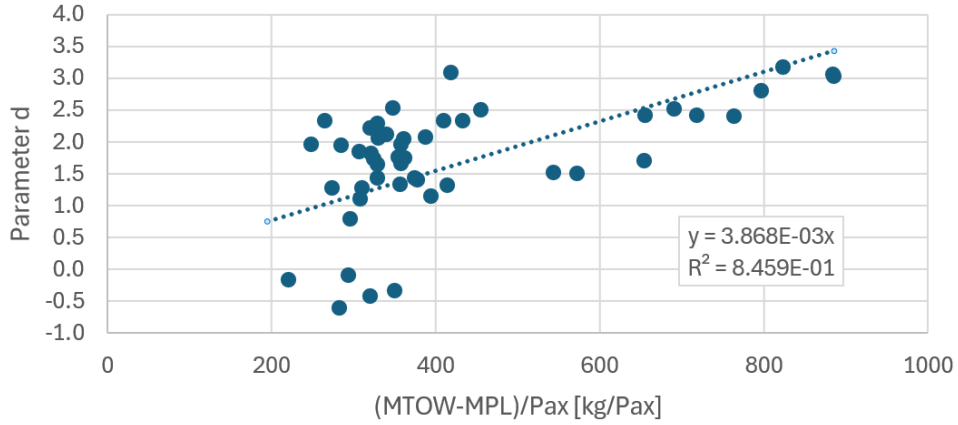

Figure 3.10 *d* versus (MTOW-MPL)/Pax of the most used passenger aircraft

No apparent relationship has been found between parameter *e* and any of the variables used in the bathtub curve calculation. However, it has been observed that for most aircraft, *e* takes negative values on the order of 10^{-4}, while for smaller aircraft – those with fewer than 50 seats – it tends to take positive values.

The approximation of the parameters is summarized in Table 3.6.

Table 3.6 Approximated parameters for the bathtub curve

Equation	R^2
$a = 4.003 \cdot \frac{MZFW - MPL}{n_{seat}}$	0.9873
$b = 6.417 \cdot \frac{MTOW - MPL}{n_{seat}}$	0.8554
$c = 1.000 \cdot R_{ferry}$	0.9987
$d = 0.003868 \cdot \frac{MTOW - MPL}{n_{seat}}$	0.8459

4 Total Fuel Consumption

The bathtub curve illustrates the fuel mass per passenger per 100 km, making it a useful tool for identifying the optimal flight distance of an aircraft. However, on its own, it does not provide information on total fuel consumption as a function of range. To determine this, the value obtained from the bathtub curve must be multiplied by the flight distance and the number of passengers.

For all the calculations performed in Chapter 3, we assumed a payload-range diagram model in which the payload is reduced first, followed by the number of passengers. The goal is to derive the equations that define the number of passengers as a function of range, which will then allow us to calculate the total fuel consumption for a given range.

4.1 Passengers as a Function of Flight Distance

In the payload-range diagram (Figure 3.1), a reduction in payload can be observed starting from point B, which increases the range up to point C, and later to the ferry range, corresponding to an aircraft without payload. This chart does not indicate what type of payload is being reduced – whether passenger load or cargo – so we will break it down below.

As mentioned before, for the payload reduction, the first mass to be reduced is cargo and then, when there is no cargo at all, passenger mass is reduced. We will call this point with zero cargo and full passengers R_D. Point R_D can be achieved between R_A and R_B or between R_B and ferry range R_C. We will call this scenario 1 and 2 respectively.

Scenario 1 occurs when the maximum passenger mass is higher than PL_B. **Scenario 2** occurs when the maximum passenger mass is lower than PL_B.

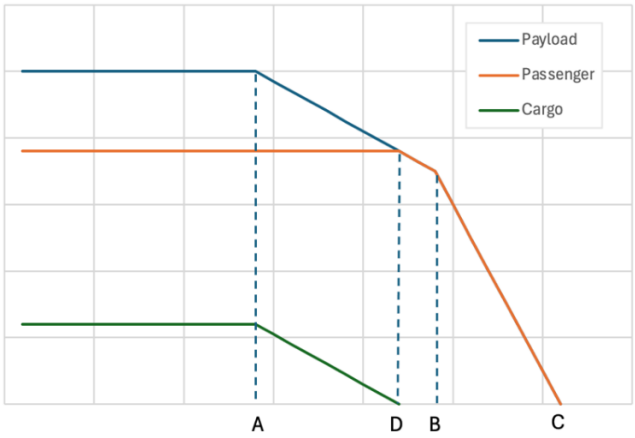

Figure 4.1 Detailed payload-range diagram for scenario 1

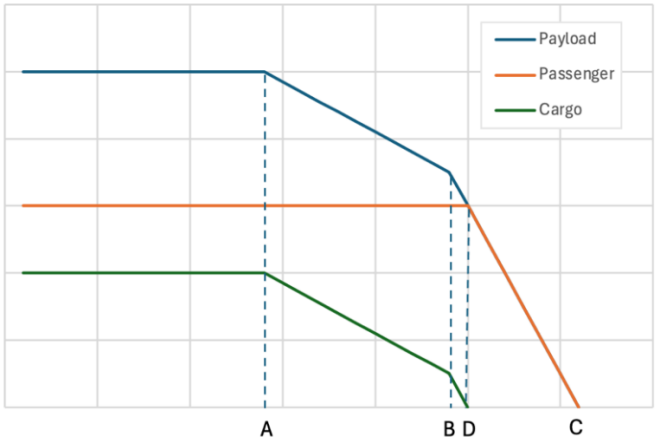

Figure 4.2 Detailed payload-range diagram for scenario 2

For both, payload can be defined as a piecewise function of flight distance.

$$PL = \begin{cases} PL_A, & 0 < R < R_A \\ PL_A - (R - R_A) \cdot \dfrac{PL_A - PL_B}{R_B - R_A}, & R_A < R < R_B \\ PL_B - (R - R_B) \cdot \dfrac{PL_B}{R_C - R_B}, & R_B < R < R_C \end{cases} \tag{4.1}$$

Payload can be defined as the sum of passenger mass and cargo.

$$PL = m_c + n_{pax} \cdot m_{pax} = m_c + m_{pass} \tag{4.2}$$

In the **first scenario**, range R_D can be found using

$$R_D = R_A - \left(n_{pax} \cdot m_{pax} - PL_A\right) \cdot \frac{R_B - R_A}{PL_A - PL_B} \quad . \tag{4.3}$$

In the first scenario, passenger mass can be written as a three parts function.

$$m_{pass} = \begin{cases} m_{pax} \cdot m_{pax}, & 0 < R < R_D \\ PL = PL_A - (R - R_A) \cdot \dfrac{PL_A - PL_B}{R_B - R_A}, & R_D < R < R_B \\ PL = PL_B - (R - R_B) \cdot \dfrac{PL_B}{R_C - R_B}, & R_B < R < R_C \end{cases} \tag{4.4}$$

In the **second scenario**, range R_D can be found using

$$R_D = R_B - \left(n_{pax} \cdot m_{pax} - PL_B\right) \cdot \frac{R_C - R_B}{PL_B} \quad . \tag{4.5}$$

In the second scenario, passenger mass can be written as a two parts function.

$$m_{pass} = \begin{cases} n_{pax} \cdot m_{pax}, & 0 < R < R_D \\ PL = PL_B - (R - R_B) \cdot \dfrac{PL_B}{R_C - R_B}, & R_D < R < R_C \end{cases} \tag{4.6}$$

Dividing the passenger mass, $m_{pass} = n_{pax} \cdot m_{pax}$ by the mass of one passenger, m_{pax}, the number of passengers for a given flight distance can be calculated for both cases.

Table 4.1 Number of passengers depending on flight distance

Case	R_D	$n_{pax}(R)$
1	$R_A - \left(n_{pax} \cdot m_{pax} - PL_A\right) \cdot \dfrac{R_B - R_A}{PL_A - PL_B}$	$\begin{cases} n_{pax}, & 0 < R < R_D \\ \left(PL_A - (R - R_A) \cdot \dfrac{PL_A - PL_B}{R_B - R_A}\right) \cdot \dfrac{1}{m_{pax}}, & R_D < R < R_B \\ \left(PL_B - (R - R_B) \cdot \dfrac{PL_B}{R_C - R_B}\right) \cdot \dfrac{1}{m_{pax}}, & R_B < R < R_C \end{cases}$
2	$R_B - \left(n_{pax} \cdot m_{pax} - PL_B\right) \cdot \dfrac{R_C - R_B}{PL_B}$	$\begin{cases} n_{pax}, & 0 < R < R_D \\ \left(PL_B - (R - R_B) \cdot \dfrac{PL_B}{R_C - R_B}\right) \cdot \dfrac{1}{m_{pax}}, & R_D < R < R_C \end{cases}$

4.2 Fuel Consumption as a Function of Flight Distance

Having the function of passengers versus flight distance, taking the values of the bathtub curve and multiplying them by the range and the number of passengers, the absolute fuel consumption for a given range is obtained.

Figure 4.3 shows the fuel consumption versus flight distance of a B737-800. It's a case of scenario 1 described in Chapter 4.1. For this diagram the values of fuel calculation with the full calculation from the Excel table have been used.

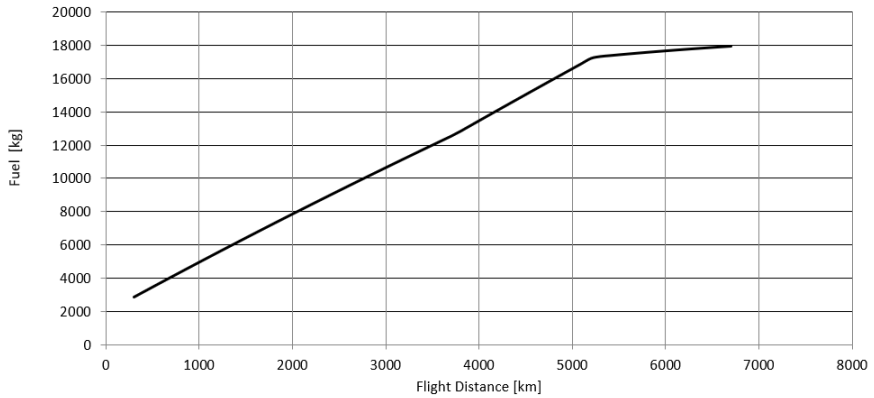

Figure 4.3 Fuel consumption versus flight distance of B737-800 using the exact values of fuel consumption

For the **calculation of a fuel consumption diagram with the analytical approximation** of the bathtub curve can also be used, instead of the full calculation, so that only the equation parameters – a, b, c, d, and e – and the characteristic points of the payload range diagram are required. Equations shown in Table 4.1 are used before the first characteristic point.

In **scenario 1**, between R_B and R_D a linear interpolation is used instead of multiplying the bathtub curve with the number of passengers and range, as this would lead to a curve that doesn't match reality (see Figure 4.6). In **scenario 2**, after R_D the absolute fuel mass can be considered constant, the limit is achieved, because the aircraft has a limited fuel tank capacity.

In **scenario 2** we apply the simplification of a constant fuel mass after R_D. Figure 4.4 shows the fuel consumption versus flight distance of a B737-800, as well as the number of passengers for every flight distance, now calculated with the analytical version of the bathtub curve.

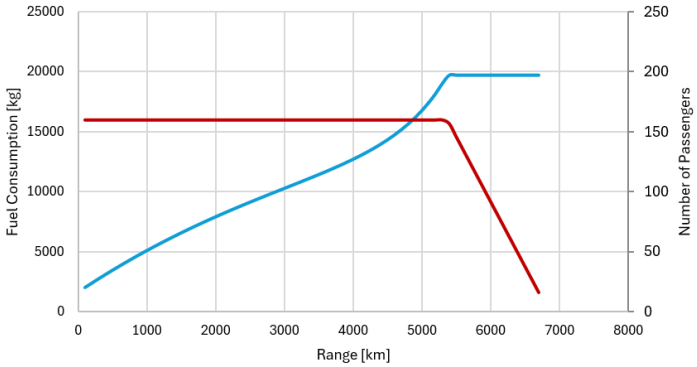

Figure 4.4 Passengers (red) and fuel consumption (blue) versus flight distance of a B737-800 (scenario 2). Fuel consumption is kept a constant mass after R_D.

For **scenario 1**, Figure 4.5 shows the fuel consumption versus flight distance of A330-200, as well as the number of passengers for every flight distance, also calculated with the analytical version of the bathtub curve. Between R_B and R_D a linear interpolation is used. After R_C the absolute fuel mass can be considered constant. The limit is achieved, because the aircraft has a limited fuel tank capacity.

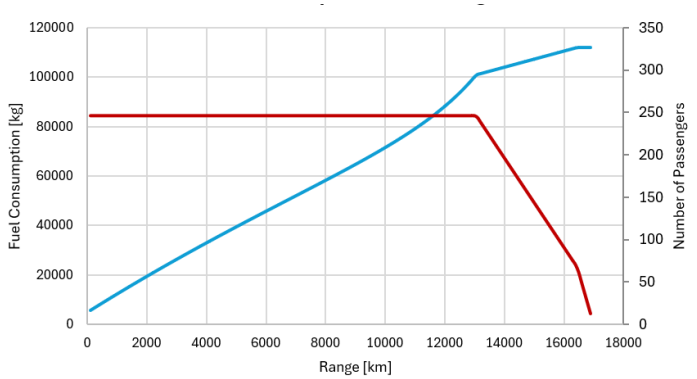

Figure 4.5 Passengers (red) and fuel consumption (blue) versus flight distance of A330-200 (scenario 1). A linear interpolation and a constant value are used.

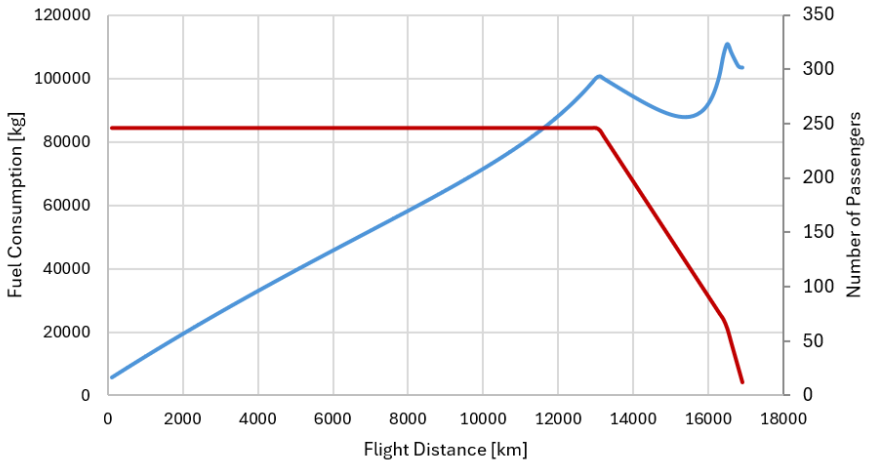

Figure 4.6 An erroneous fuel consumption chart results for flight distances larger than R_D, when simply taking the values of analytical version of the bathtub curve and multiplying them by the range and the number of passengers to get the absolute fuel consumption. Shown is the example of the A330-200. Instead, between R_B and R_D a linear interpolation must be used. After R_C the absolute fuel mass must be considered constant. This is done in Figure 4.5.

5 Intermediate Stop Operation (ISO)

As an extension of the discussion on flight efficiency and fuel planning, this section examines the concept of Intermediate Stop Operations (ISO) – a flight strategy in which a long route is divided into two segments, with a stop for refueling.

Although not common in regular commercial service, ISO can be considered in specific cases where range limitations, payload constraints, or fuel efficiency make a continuous flight less practical. This brief analysis outlines the basic principles of ISO and evaluates its potential advantages and trade-offs in comparison to direct, single-stage operations.

In evaluating the feasibility and efficiency of Intermediate Stop Operations, this study will not only assess fuel consumption but also consider the economic and operational implications. One key aspect is the possibility of utilizing smaller, more fuel-efficient aircraft for each flight segment, which may offer cost advantages compared to operating a single larger aircraft across the entire route. This approach could potentially optimize fleet usage, lower emissions per seat-kilometer, and improve route flexibility.

Additionally, the practical implementation of ISO must account for regulatory and legal considerations, particularly those related to the International Civil Aviation Organization's (ICAO) Freedoms of the Air. These govern a state's right to enter and operate within the airspace and airports of other countries.

5.1 Potential ISO Routes and Aircraft

We will first identify and evaluate a potential route and suitable aircraft configurations where Intermediate Stop Operations (ISO) may offer practical or economic advantages.

The London–Perth connection has been selected as a relevant case study. Currently operated by Qantas as flight QFA9, this ultra-long-haul route is among the longest nonstop commercial flights in the world. Covering an actual distance of 15,190 km with a total flight time of approximately 17 hours, it serves as an ideal candidate for evaluating the technical feasibility and economic efficiency of implementing alternative operational models such as ISO on extended intercontinental services. Flight data is specified in Table 5.1.

Table 5.1 Flight information of QFA9

	QFA9
Took-off from	Perth, Australia (PER)
Landed at	London, UK (LHR)
Take-off time	WED 02-07-2025 02:17 AM AWST
Landing time	WED 02-07-2025 12:21 PM BST
Total trip time	17 h 4 min
Airline	Qantas
Aircraft	Boeing 787-9 Dreamliner
Actual distance	15,190 km
Direct distance	14,525 km

The bathtub curve for the Boeing 787-9 used in this route is shown in Figure 5.1. As can be appreciated, minimum fuel stage length is 14,800 km, where the fuel per range and passenger is 2.14 kg/Pax/100 km. For the route studied, the aircraft is operating after its optimal point, where the fuel consumption starts to increase.

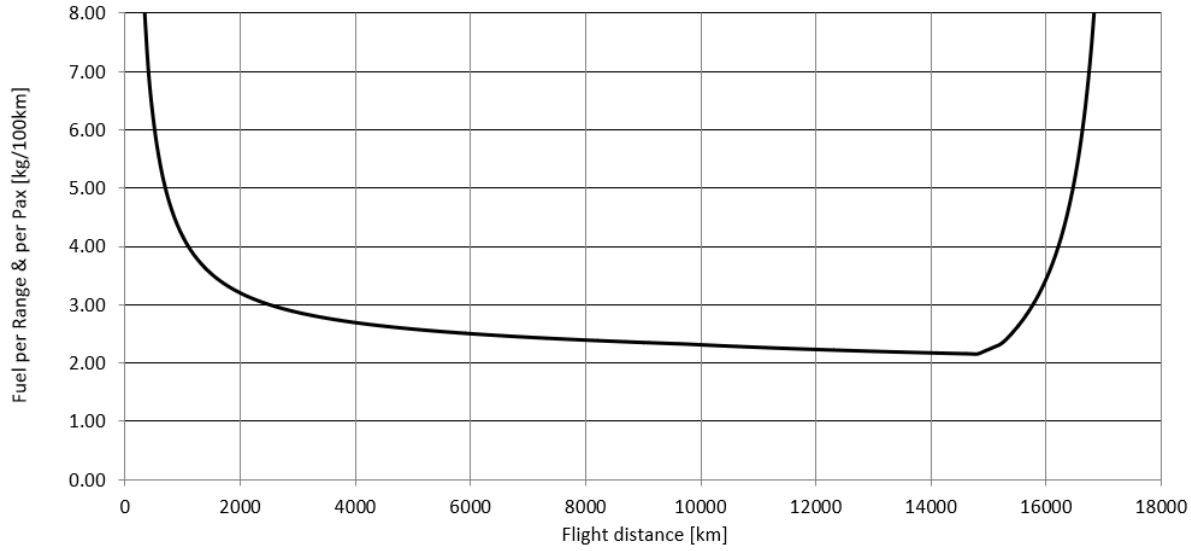

Figure 5.1 Bathtub curve of the Boeing 787-9

The Boeing 787-9 has a total of 290 seats. When operating the route under study, the aircraft must fly with a reduced payload, limiting the maximum number of passengers to 268. In other words, it cannot operate with a Passenger Load Factor (PLF) of 1; the highest possible PLF is 0.92.

For the defined route and using the actual distance, we can calculate the absolute value of the fuel consumption, which results in 94,129 kg. Dividing by the number of passengers, we can obtain the fuel per passenger, 351.22 kg/Pax. According to the analytical bathtub curve and using the Easy Consumption Excel Table, the fuel consumption per passenger and 100 km is 2.31 kg.

To simplify the study, we will assume that an ISO is carried out by dividing the total distance into two equal legs of 7,595 km which would correspond to a stopover in Dubai, approximately halfway (see Figure 5.2). We will perform the same calculation again using the same aircraft.

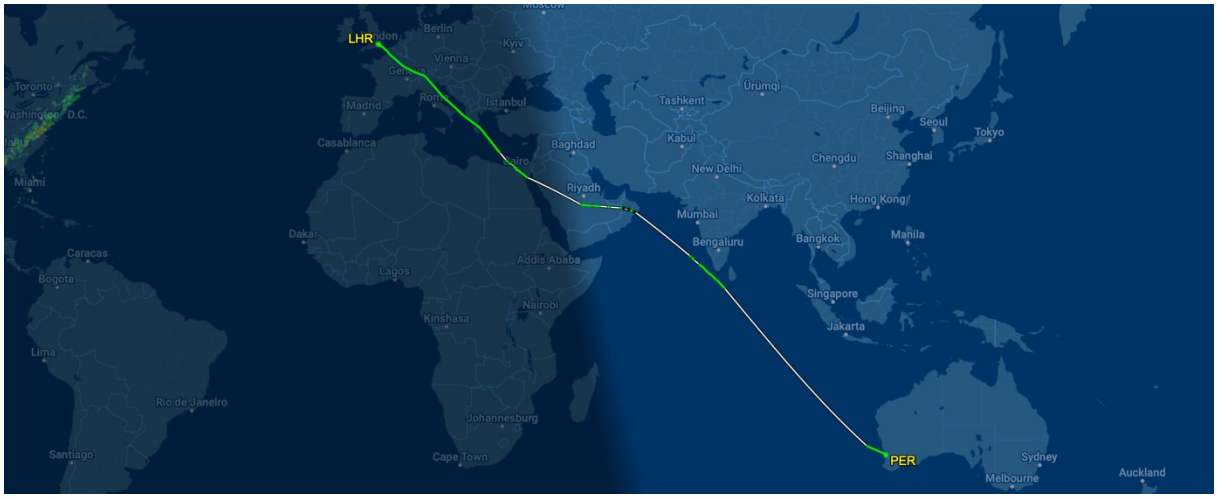

Figure 5.2 Flight QFA of the 2nd of July 2025 from (Flightaware 2025)

The fuel consumption of each leg is now 52,921 kg. However, since we are operating in a region further to the left on the payload-range diagram, a PLF of 1 can be achieved. The total fuel consumption for the full journey, considering both stages, amounts to 105,842 kg. When divided by the 290 passengers, this results in 364.97 kg/Pax, and by the flight distance 2.40 kg/Pax/(100 km). Despite the ability to increase the number of passengers to the aircraft's full capacity, the overall fuel consumption has increased compared to the direct flight.

A different approach of the ISO would be using a different aircraft, more suitable for the reduced distance. Using the Fuel per Passenger Excel Table we can find the least consuming aircraft for the desired flight distance, in our case 7,595 km.

The most suitable airplane for this leg of the route, with a fuel consumption per passenger of 121.89 kg/Pax, is the Boeing 777-200ER. Though it may seem unintuitive, extended range versions of aircraft have been used for shorter distances for their good performance. Using the B777-200ER, the absolute fuel consumption for each leg is 45,667 kg, 91,334 kg for the whole route. The route could be operated with 375 passengers, so the fuel consumption per passenger would be 243.56 kg/Pax, 1.60 kg/Pax/(100 km). Figure 5.3 shows the bathtub curve of the Boeing 777-200ER. As it can be seen in the bathtub curve, for the stage length desired, the airplane operates before it's minimum stage length.

It may seem that the solution to reduce fuel consumption on this route is to perform an ISO using a different aircraft. However, another possibility should also be considered: that the Boeing 777-200ER might be even more efficient when operating a direct flight. If we look at the absolute fuel consumption, we see that the fuel needed for the direct flight with the 777-200ER is 87,593 kg. Although the absolute fuel is lower than with the ISO, the number of

passengers has to be reduced to 333 to achieve the whole length of the trip, so the fuel per passenger is slightly higher, 263.04 kg/Pax. This can also be seen in the bathtub curve, as the distance between Perth and London is achieved after the minimum fuel stage length, where the fuel consumption increases rapidly. The results are listed in Table 5.2.

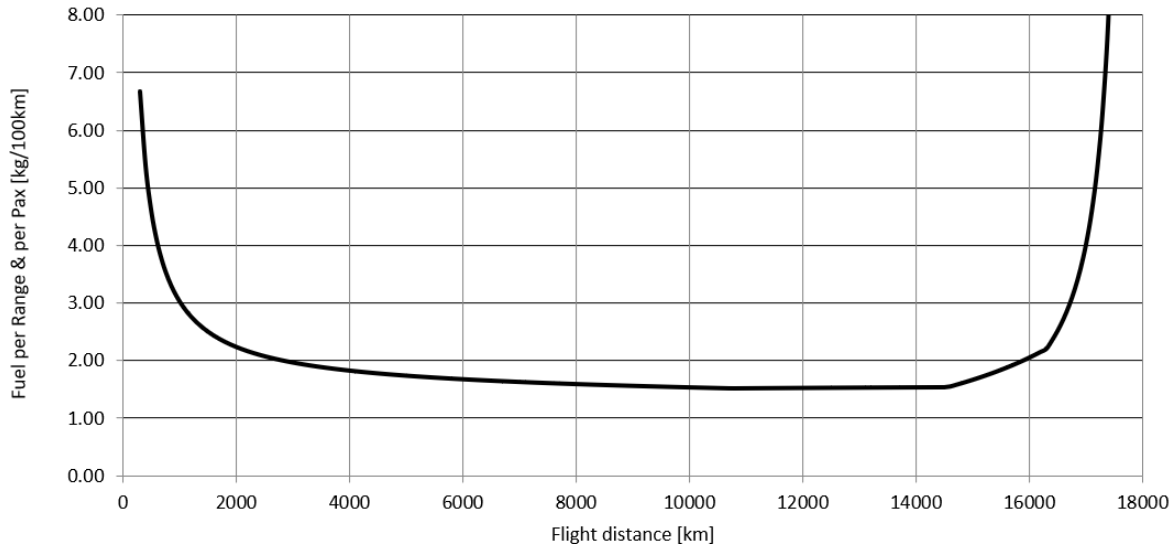

Figure 5.3 Bathtub curve of the Boeing 777-200ER

Table 5.2 ISO comparison for the route Perth-London

	B787-9	B787-9 (ISO)	B777-200ER (ISO)	B777-200ER
Total Fuel [kg]	94,129	105,842	91,334	87,593
Change Percentage [%]	0	+12.44	-2.97	-6.94
Number of Passengers	268	290	375	333
Fuel per Passenger [kg/Pax]	351.22	364.97	243.56	263.04
Change Percentage [%]	0	+3.91	-30.65	-25.11
Fuel Consumption [kg/Pax/100km]	2.31	2.40	1.60	1.73
Change Percentage [%]	0	+3.9	-30.7	-25.1

As a conclusion of the case study, we can state that performing an Intermediate Stop Operation can lead to a higher fuel consumption, but if it is done with an aircraft especially selected for the stage length, the total fuel consumption can be reduced by 2.97% and the fuel consumption per passenger by 30.7%. The B777-200ER could have been used in the first place. The fuel consumption per passenger and 100 km could have been reduced from 1.73 kg/100 km to 1.60 kg/100 km. This is a **reduction of 7.5%**.

5.2 Practical Implications

Making an intermediate stop instead of operating a long-haul direct flight involves several practical disadvantages that must be carefully considered.

First, operating costs increase significantly. Landing at an additional airport entails paying landing fees, handling services, security charges, and possibly parking fees. Moreover, operations must be coordinated at a second airport, requiring more personnel, additional logistical support, and more complex planning. These factors raise the overall cost of the journey, even if fuel consumption per passenger may be reduced.

Another important aspect is the increase in total travel time. While each leg may be more fuel-efficient on its own, the time required for landing, refueling, and taking off again adds a delay that can affect the competitiveness of the route. This is particularly relevant for intercontinental flights, where passengers often prefer quick connections or nonstop service for reasons of comfort and fatigue.

From the passenger's perspective, the experience is also affected. Flights with stopovers are generally less appealing than direct flights, as they involve longer travel times, possible layovers at intermediate airports, and greater exposure to delays or operational issues. On long-haul routes, where rest is especially important, a stop halfway through can be inconvenient and tiring.

In addition, the environmental and social impact must be considered. The take-off and landing phases are the most fuel- and emission-intensive segments of a flight, per minute. Doubling these phases may increase the environmental footprint, even if total fuel consumption per passenger drops slightly compared to a direct flight, as the damage is caused nearer to the surface. Furthermore, each take-off and landing contributes significantly to aircraft noise, which directly affects communities living near airports. This noise can have negative consequences on public health and quality of life, especially in densely populated areas.

5.3 Regulatory Considerations

To operate an ISO it is necessary, as a minimum, to have the right to land at an intermediate airport for refueling. This stop does not involve boarding or disembarking passengers or cargo and is therefore considered a technical stop.

For this reason, the operation requires the use of the Second Freedom of the Air.

> ***Second Freedom of the Air*** *– the right or privilege, in respect of scheduled international air services, granted by one State to another State or States to land in its territory for non-traffic purposes (also known as a Second Freedom Right). (ICAO, 2025)*

Since ISO operations are intended for long-haul flights, it is also common to overfly multiple countries. As such, the First Freedom of the Air is also required.

> ***First Freedom of the Air*** *– the right or privilege, in respect of scheduled international air services, granted by one State to another State or States to fly across its territory without landing (also known as a First Freedom Right). (ICAO, 2025)*

Because the operation involves international flights, passengers must be boarded and disembarked in both the airline's home country and the foreign destination. Therefore, the Third and Fourth Freedoms of the Air are also necessary.

> ***Third Freedom of the Air*** *– the right or privilege, in respect of scheduled international air services, granted by one State to another State to put down, in the territory of the first State, traffic coming from the home State of the carrier (also known as a Third Freedom Right). (ICAO, 2025)*

> ***Fourth Freedom of the Air*** *– the right or privilege, in respect of scheduled international air services, granted by one State to another State to take on, in the territory of the first State, traffic destined for the home State of the carrier (also known as a Fourth Freedom Right). (ICAO, 2025.)*

Additionally, since the airline's home country is one end of the route and the technical stop occurs in a third country, it may be desirable to sell seats between the stopover and the final destination in order to maximize profitability. This would require the Fifth Freedom of the Air.

> ***Fifth Freedom of the Air*** *– the right or privilege, in respect of scheduled international air services, granted by one State to another State to put down and to take on, in the territory of the first State, traffic coming from or destined to a third State (also known as a Fifth Freedom Right). (ICAO, 2025)*

A total of 79 states signed the International Air Services Transit Agreement (UN 2025). This agreement implies that all signatory countries grant each other the first two freedoms of the air automatically, meaning ISO would be possible between them if also the fourth and fifth freedoms are granted with a bilateral agreement.

This is based on the assumption that the airline conducting the ISO (Intermediate Stop Operation) is based at one end of the route. In such a scenario, the airline must navigate a more complex regulatory environment, requiring overflight rights (first freedom), technical landing rights (second freedom), and traffic rights (third, fourth, and ideally fifth freedom) in at least three different states: the home country, the technical stop country, and the destination country. These requirements make coordination more difficult and reduce route flexibility, especially when bilateral air service agreements are limited or politically sensitive.

However, the operational and regulatory complexity is significantly reduced when the airline is based at or near the midpoint of the route. In such cases the airline's home base can serve both as a refueling stop and as a traffic-handling hub. This setup often allows for easier compliance with international agreements and more efficient route planning.

According to Ellis (2019), an example of this strategic advantage can be seen with the Gulf carriers, Emirates (UAE), Qatar Airways (Qatar), and Etihad (UAE), which have experienced a rise over the last decade. Located geographically between Europe and Asia-Pacific or Africa,

these airlines operate extensive networks using their home hubs (e.g., Dubai, Doha, Abu Dhabi) as technical and traffic points. Since their base lies in the middle, these airlines can consolidate traffic flows from multiple origin and destination pairs, reducing the need for additional technical stops.

As explained in Aviation Strategy (2017), another excellent case is Icelandair, which uses Keflavík International Airport (KEF) as a natural midpoint between North America and Europe. While technically a small carrier, Icelandair has developed a successful hub-and-spoke model where passengers can transfer between North American and European cities via KEF. Because Iceland is conveniently positioned in the North Atlantic, it can offer competitive transatlantic flights with relatively short flying distances and fewer legal complications.

Thus, when an airline is geographically situated between major global regions, ISO becomes not just viable but commercially advantageous. It minimizes dependency on complex bilateral agreements and enables the airline to better control the network and passenger flow. This positioning can be a powerful enabler for building a global hub.

5.4 Evaluation of Trade-offs

The analysis of Intermediate Stop Operations (ISO) in the context of ultra-long-haul flights, specifically the Perth–London route, demonstrates that this operational model can provide significant improvements in fuel efficiency per passenger, but only under specific conditions. The case study shows that when a suitable aircraft is carefully selected for each leg, an ISO strategy may outperform a single-stage operation in terms of fuel consumption per passenger. In particular, the Boeing 777-200ER operating a two-leg journey with a technical stop in Dubai yielded a notably lower fuel consumption per passenger compared to both the direct operation with the same aircraft and the original Boeing 787-9 configuration.

However, this benefit comes with several trade-offs. Operational complexity increases due to the need for coordination at an additional airport, and economic costs rise from airport fees and ground handling services. Moreover, passenger experience may be negatively affected by longer travel times and reduced convenience compared to direct services.

In regulatory terms, ISO requires careful navigation of international airspace agreements. Access to the First and Second Freedoms of the Air is essential for technical stops, while broader operational and commercial opportunities – such as picking up or dropping off passengers at the stopover– require the granting of additional freedoms. These legal prerequisites may limit the applicability of ISO to specific routes and geopolitical contexts.

Environmental and social considerations also weigh heavily. Though ISO may reduce emissions per passenger in optimized scenarios, the additional noise impact on airport-adjacent communities, caused by duplicated take-off and landing cycles, cannot be overlooked.

This concern is reflected in the environmental rating methodology proposed by Scholz and students at HAW Hamburg, the Ecolabel for Aircraft. where a weighted summation type is used to calculate an aircraft's ecological impact. The model adds up fuel consumption, CO_2 equivalents, local noise, and air pollution, normalizing each against a reference flight (2400 km on a Boeing 737-800), and combines them into a composite score.

> *The "summation type" calculator is adding up fuel consumption, equivalent CO2, local noise level, and local air pollution and sets it in relation to the values from a standard flight (defined as 2400 km flown with a Boeing 737-800). This can be done for one, two, three, or four flights. The longer the total flight, the worse the score. Noise and local air pollution add up with every take-off and landing (i.e. with each flight). For this reason, it tends to be better for the environment to reach the final destination in a single flight. (Scholz, 2025)*

Within the Ecolabel research, in the summary of his project, Rösing (2021) concludes that flights with fewer layovers tend to receive higher ratings, while those with more layovers are usually rated the lowest, largely due to the additional noise and air pollution generated by each take-off and landing.

> *In 9 out of 10 investigated pairs of origin and destination, the flight option with less layovers was always the one with the best and the flight option with the most layovers was always the one with the worst rating. Every start and landing causes additional noise and air pollution at the environment of an airport, this leads to worse ratings and only in one contemplated example the aircraft on a direct flight was worse rated than a flight with a layover. (Rösing, 2021)*

In summary, while ISO represents a potentially viable strategy for improving efficiency on very long routes, its implementation is not universally advantageous. The decision to adopt such a model must be based on a detailed case-by-case analysis that incorporates fuel performance, aircraft capability, operational costs, passenger demand, regulatory feasibility, and environmental externalities.

6 Users Guide for the Excel Tables

6.1 Calculation of the Parameters of the Bathtub Curve

The Fuel Consumption Excel Table is a tool that expands the Burzlaff 2017 spreadsheet in order to obtain the parameters that define the analytical bathtub curve. Below, the instructions on how to use it are exemplified with the calculation for Airbus A320neo.

Aircraft data must be entered into the cells with a white background (see Figure 6.1). The required inputs include characteristic masses, points from the payload-range diagram, the number of seats, distance to alternate, and the flight Mach number, which can all be found in the Airport Planning Manuals given by the manufacturers.

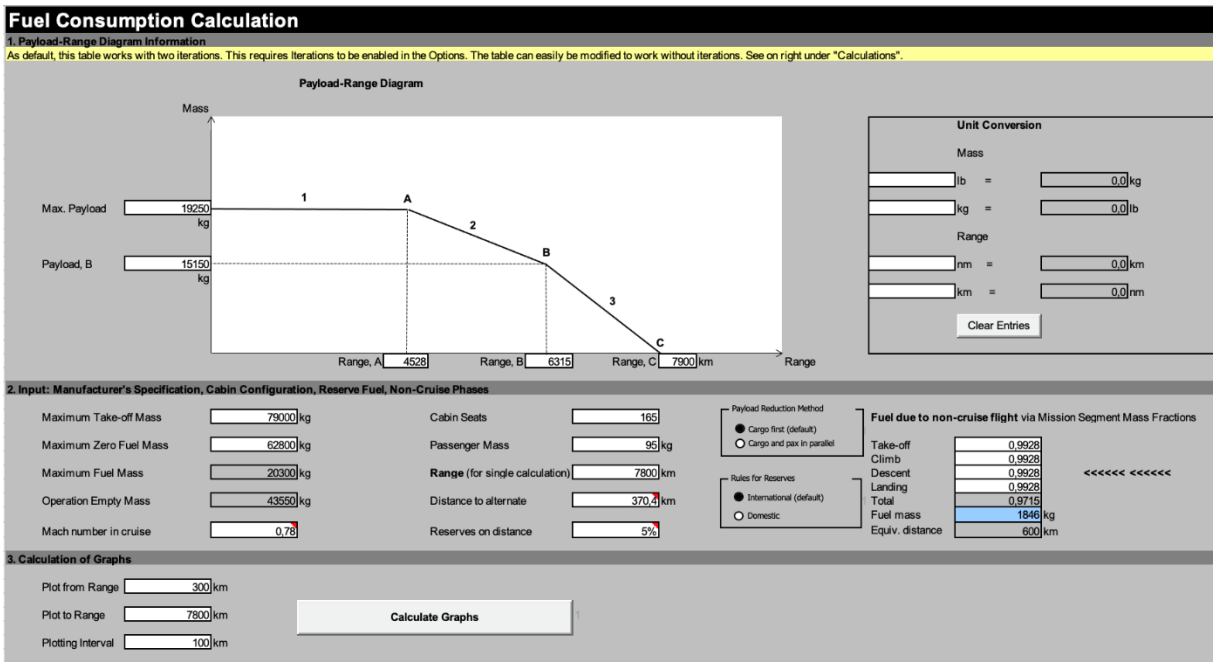

Figure 6.1 Inputs of the Fuel Consumption Excel Table

Once the data is entered, you must press the Calculate Graphs button and wait until cell I33 (*Range for single calculation*) reaches the value in cell C43 (*Plot to Range*).

In the extended section of the spreadsheet, starting at cell AI42, you should enter the initial values for the parameters *a, b, c, d,* and *e*, which will approximate the bathtub curve. It is very important to ensure these values are close to the desired final solution to avoid errors. A good starting point is to enter values previously obtained for a similar aircraft, use the ferry range value for parameter *c*, 0 for parameter *e* and a value between 1 and 3 in parameter *d* (see Figure 6.2).

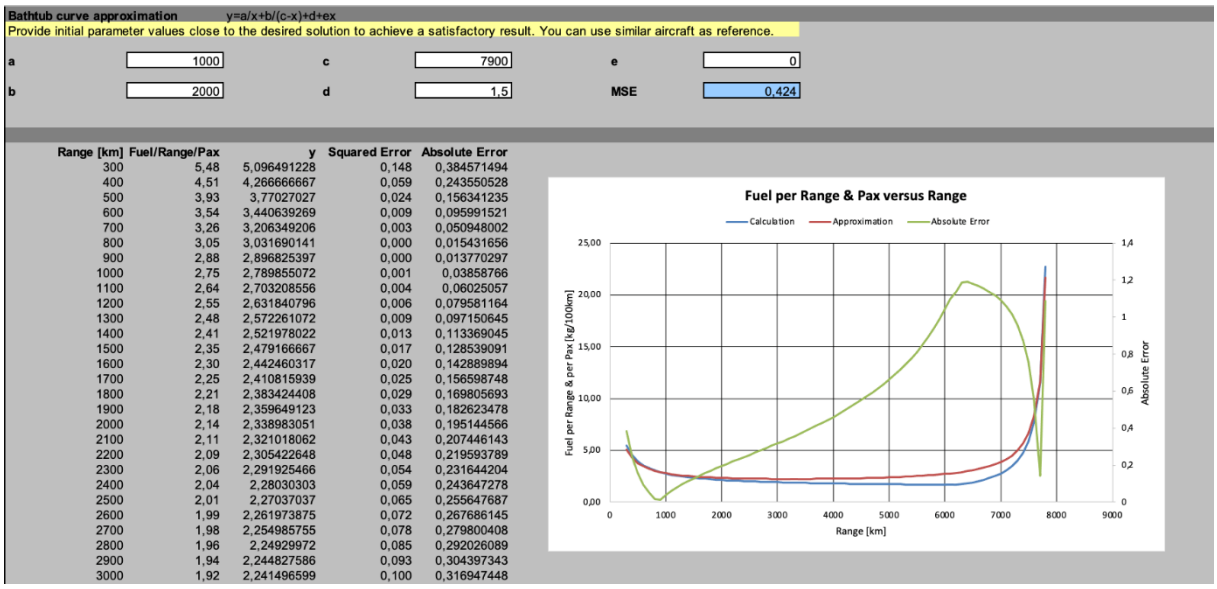

Figure 6.2 Inputs for the approximation of the bathtub curve

In cell AO44, you will find the Mean Squared Error (MSE). You must select it and use Excel's Solver to find the optimal solution choosing the options shown in Figure 6.3.

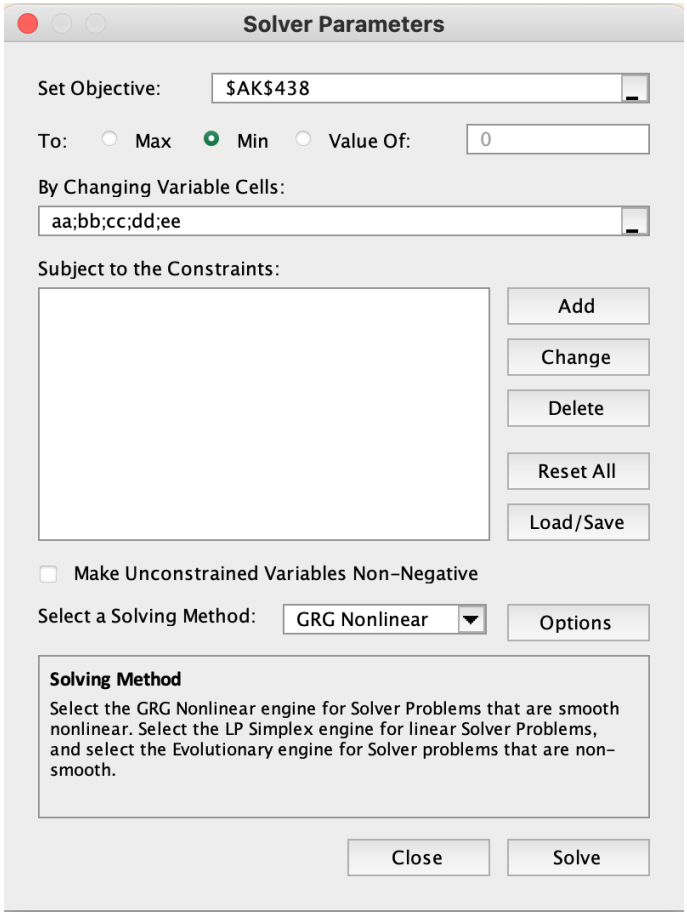

Figure 6.3 Solver parameters

Once the process is complete, select the option *Keep Solver Solution* and *OK* (see Figure 6.4).

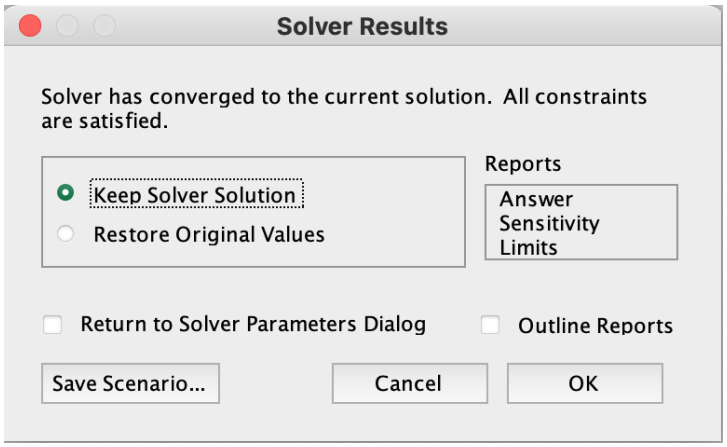

Figure 6.4 Solver results

In the same cells where we enter the initial values of the parameters that define the analytical version of the bathtub curve, we find the new optimized parameters that minimize the MSE. As can be seen in Figure 6.5, the approximated curve and the one obtained through the full iterative calculation match.

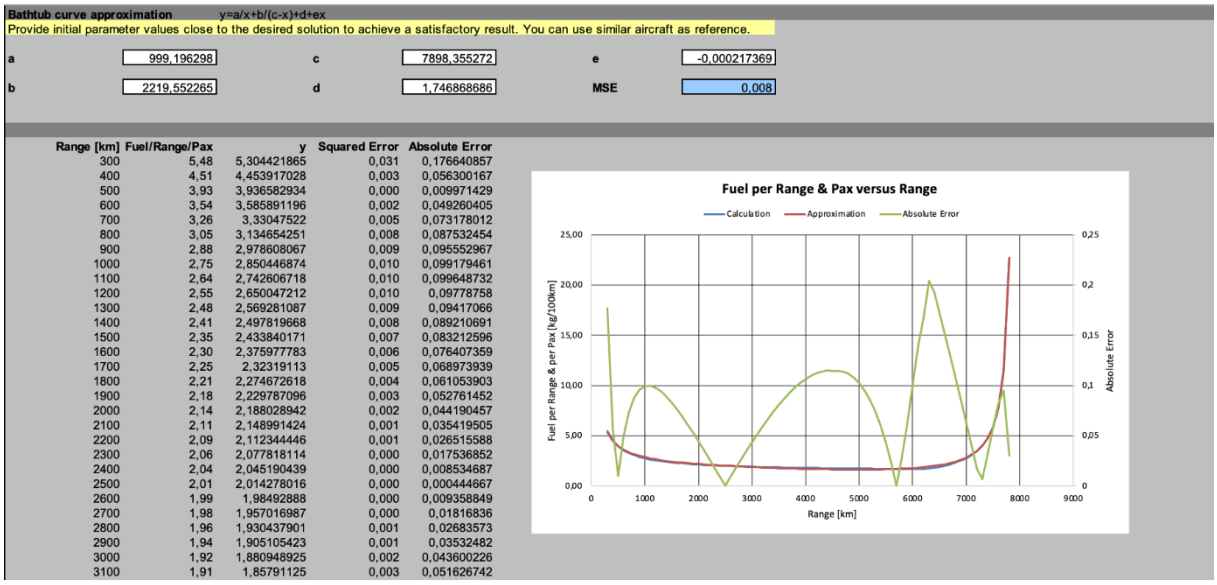

Bathtub curve approximation y=a/x+b/(c-x)+d+ex

Provide initial parameter values close to the desired solution to achieve a satisfactory result. You can use similar aircraft as reference.

a	999,196298	c	7898,355272	e	-0,000217369
b	2219,552265	d	1,746868686	MSE	0,008

Range [km]	Fuel/Range/Pax	y	Squared Error	Absolute Error
300	5,48	5,304421865	0,031	0,176640857
400	4,51	4,453917028	0,003	0,056300167
500	3,93	3,936582934	0,000	0,009971429
600	3,54	3,585891196	0,002	0,049260405
700	3,26	3,33047522	0,005	0,073178012
800	3,05	3,134654251	0,008	0,087532454
900	2,88	2,978608067	0,009	0,095552967
1000	2,75	2,850446874	0,010	0,099179461
1100	2,64	2,742606718	0,010	0,099648732
1200	2,55	2,650047212	0,010	0,09778758
1300	2,48	2,569281087	0,009	0,09417066
1400	2,41	2,497819668	0,008	0,089210691
1500	2,35	2,433840171	0,007	0,083212596
1600	2,30	2,375977783	0,006	0,076407359
1700	2,25	2,32319113	0,005	0,068973939
1800	2,21	2,274672618	0,004	0,061053903
1900	2,18	2,229787096	0,003	0,052761452
2000	2,14	2,188028942	0,002	0,044190457
2100	2,11	2,148991424	0,001	0,035419505
2200	2,09	2,112344446	0,001	0,026515588
2300	2,06	2,077818114	0,000	0,017536852
2400	2,04	2,045190439	0,000	0,008534687
2500	2,01	2,014278016	0,000	0,000444667
2600	1,99	1,98492888	0,000	0,009358849
2700	1,98	1,957016987	0,000	0,01816836
2800	1,96	1,930437901	0,001	0,02683573
2900	1,94	1,905105423	0,001	0,03532482
3000	1,92	1,880948925	0,002	0,043600226
3100	1,91	1,85791125	0,003	0,051626742

Figure 6.5 New parameters for the approximation of the bathtub curve

This process has been carried out for the 50 most commonly used passenger aircraft according to Kühn (2023). The results can be found in the Excel table Parameters of the bathtub curve (Parameters_Bathtub_Curve.xlsx) and in Appendix B.

6.2 Easy Calculation of the Bathtub Curve

The Easy Consumption Excel Table (Easy_Consumption.xlsx) is a tool that plots the analytical version of the bathtub curve, as well as the absolute fuel consumption. Its use is explained below with data of Airbus A330-200 as an example.

As input data, it uses the calculated parameters for the approximation, which are listed in the Excel table "Parameters of the Bathtub Curve" (Parameters_Bathtub_Curve.xlsx) and in Appendix B.

For the bathtub curve only the *a, b, c, d* and *e* parameters are needed, the masses, payload-range diagram and number of seats are just necessary for the absolute fuel consumption.

In order to also obtain the point where the minimum fuel consumption is achieved, an initial estimate x_{min} within the possible ranges has to be written in the corresponding cell.

All the values have to be introduced in the white background cells, as seen in Figure 6.6.

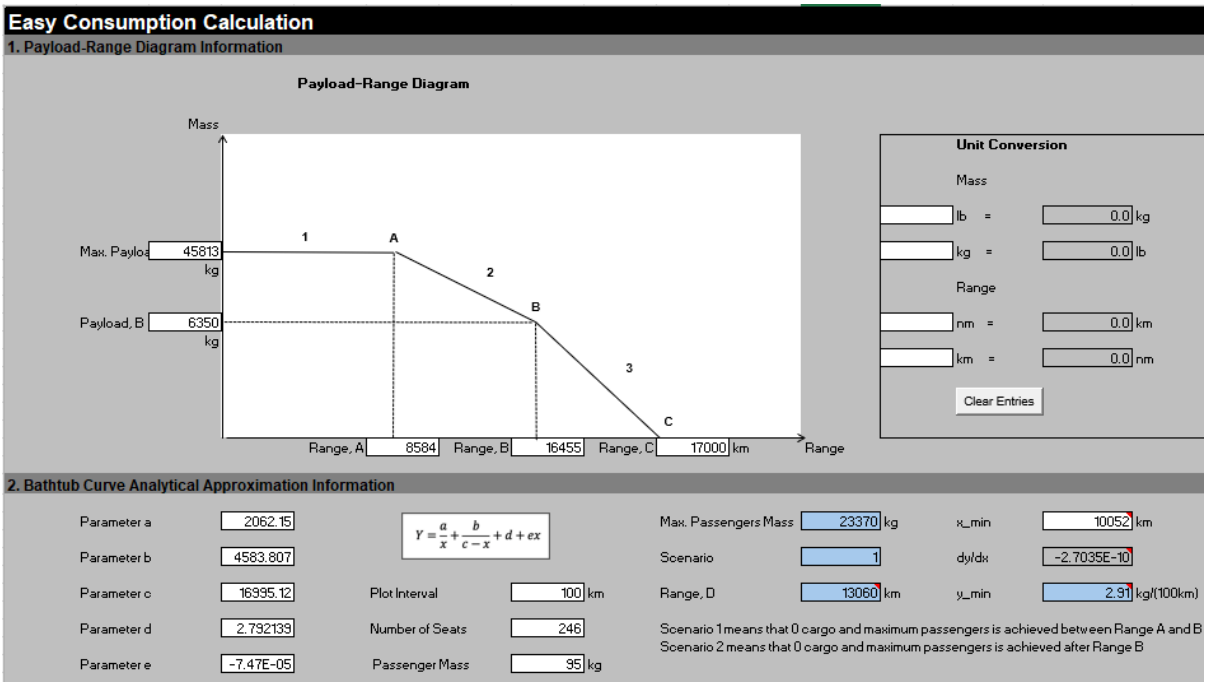

Figure 6.6 Input data for the Easy Consumption Excel

To calculate the minimum fuel stage length, we equal the derivate of the bathtub curve, *dy/dx*, to 0 by selecting cell O30 and using the Solver to drive this value to zero, using as a variable the flight distance (xx in the Excel).

$$\frac{dy}{dx} = -\frac{a}{x^2} + \frac{b}{(c-x)^2} + e = 0 \tag{6.1}$$

After introducing all the data mentioned before and choosing a suitable plot interval, we obtain the bathtub curve approximation with the minimum fuel stage length (see Figure 6.7) and the absolute fuel consumption (see Figure 6.8). For a better understanding of the relationship between fuel consumption and the payload-range diagram, the number of passengers for every range is also shown on the diagram using a secondary axis.

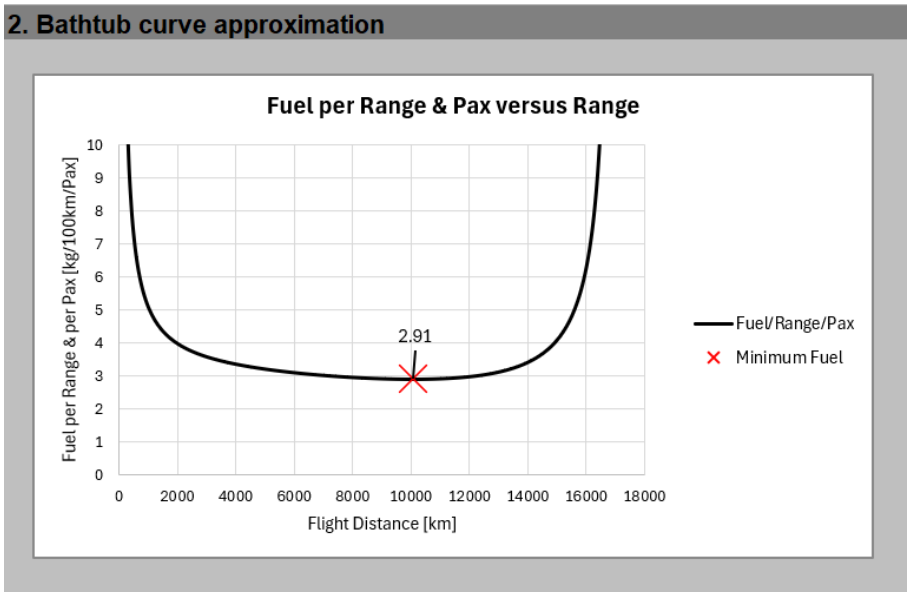

Figure 6.7 Bathtub curve approximation

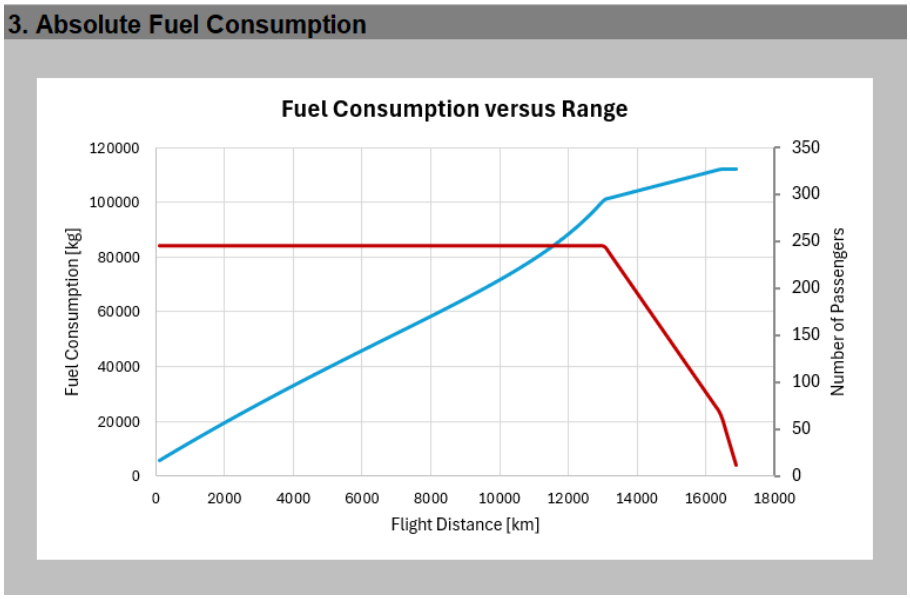

Figure 6.8 Absolute fuel consumption and number of passengers

Appendix B shows for all 50 aircraft: The fuel consumption at R_A (kg/100 km), the minimum fuel consumption determined with the analytical bathtub curve (kg/100 km), the stage length or flight distance at this minimum fuel consumption, and the difference (%) of the two fuel consumptions. The results can also be found in the Excel table with Parameters of the bathtub curve (Parameters_Bathtub_Curve.xlsx).

6.3 Aircraft Selector for a Specific Route

The Fuel per Passenger Calculator Excel Table (Fuel_Pax_Calculator.xlsx) is a tool that uses the parameters of the analytical bathtub curve to calculate the fuel consumption per passenger for a given flight distance.

By introducing a certain flight distance in cell B2, the fuel per passenger in kg/pax is given for each aircraft from the list. Using conditional format, each value gets graded in colors on a scale from green to red, green meaning the lowest fuel consumption – and therefore the most suitable aircraft for the given range– and red the highest fuel consumption.

If an airplane's ferry range is shorter than the input flight distance, then the message *Out of range* is shown instead of the consumption per passenger value.

Although this Excel table may be useful to choose the least consuming aircraft for a given flight distance, for further information such as real number of passengers or absolute fuel consumption the two Excel tables mentioned in the previous sections should be used – the Easy Consumption Excel Table and the Fuel Consumption Excel Table.

For example, as seen in Figure 6.9, introducing a desired flight distance of 1500 km, the most suitable airplane is Boeing B737-900, the least suitable the Beechcraft 1900D – which would be operating near to its ferry range–, and one airplane cannot even reach the desired flight distance.

Desired stage length	1500	(km)												
Aircraft Type	Max. Payload (kg)	Payload, B (kg)	Range A (km)	Range B (km)	Range C (km)	MTOM (kg)	MZFM (kg)	Cabin Seats	a	b	c	d	e	Total Fuel per Passenger (kg/Pax)
Airbus A220-300	12300	6513	3889	6945	8241	67585	55792	140	1348,12	3337,498	8233,765	1,137542	-7,4E-05	36,31
Airbus A319	17400	15600	4630	5413	7300	75500	58500	134	1113,754	2519,369	7297,2	2,320599	-0,00031	45,55
Airbus A320	19750	16125	3882	5200	6800	78000	62500	150	1089,05	2243,804	6797,39	2,066881	-0,0003	41,57
Airbus A320neo	19250	15150	4528	6315	7900	79000	62800	165	999,1963	2219,552	7898,355	1,746869	-0,00022	36,51
Airbus A321	24242	20152	4215	5460	7500	93500	77800	185	1156,737	2235,462	7500,231	1,428959	-0,0002	34,12
Airbus A321neo	23950	21350	5649	6482	8500	97000	73300	206	920,1342	2444,507	8498,744	1,757143	-0,0002	36,27
Airbus A330-200	45813	6350	8584	16455	17000	242000	170000	246	2062,15	4583,807	16995,12	2,792139	-7,5E-05	65,26
Airbus A330-300	45359	34927	7723	10038	16500	242000	175000	300	1571,746	7785,797	16501,84	2,407118	-0,00015	56,24
Airbus A330-900	45813	5000	7723	17372	18000	242000	181000	300	1945,753	6123,728	17999,28	1,697017	-3,4E-05	49,71
Airbus A350-900	53700	24800	10797	15890	18000	280000	195700	315	1629,386	4438,5	17994,37	2,40892	-0,00011	54,04
Airbus A380-800	83571	34286	12131	16298	17900	575000	369000	555	1726,007	5481,708	17893,63	3,021295	-0,00013	64,71
ATR 42	5045	2455	969	3034	3241	18600	16700	48	1398,631	78,22654	3128,554	-0,60933	0,001502	39,35
ATR 72	7000	4000	926	3087	3426	22500	20500	70	1021,195	213,7266	3339,15	-0,16216	0,000892	29,59
Beechcraft 1900D	2189	1896	256	707	2306	7764	7120	19	-1123,24	3736,178	2325,594	5,924449	-0,00295	79,24
Boeing 717-200	12020	8431	2185	3704	4630	49895	42638	106	1196,829	1957,911	4626,63	1,328936	-0,00028	34,95
Boeing 737 Max 8	20930	16983	4842	6426	8150	82190	65952	162	1225,962	1539,87	8125,802	1,402081	-7,2E-05	35,16
Boeing 737 MAX 9	23791	20480	4630	5843	7780	88314	70987	180	1059,145	1931,275	7766,192	1,656001	-0,0002	35,66
Boeing 737-300	15435	10763	3439	5159	6700	61235	48308	128	1032,589	3189,812	6701,819	1,956025	-0,00031	41,99
Boeing 737-400	19979	15478	3258	4630	6200	68039	53070	146	938,4823	2594,422	6198,833	2,286154	-0,00037	43,75
Boeing 737-500	15356	10022	2910	4994	6570	60555	46493	108	1105,159	3838,041	6567,75	3,077357	-0,00047	57,94
Boeing 737-700	17554	11589	3945	6186	7408	70080	55202	128	1127,719	2286,309	7400,533	2,329962	-0,00027	45,88
Boeing 737-800	21184	16716	3750	5223	6850	79015	62731	160	1036,46	2331,888	6843,216	2,042166	-0,00028	41,15
Boeing 737-900	19832	15273	3704	5149	6575	74389	62731	177	1003,043	1924,906	6576,117	1,102335	-0,00018	28,15
Boeing 747-400	67298	23800	10570	13100	15280	396893	246073	400	1594,238	10245,16	15286,41	3,166111	-0,00023	69,47
Boeing 757-200	22628	13178	4321	6482	8000	99790	83461	186	1278,177	3413,189	8001,382	1,303914	-0,00016	36,64
Boeing 767-300	40029	22793	4260	7778	9445	158757	126098	261	1198,457	3318,108	9436,646	2,588839	-0,00024	51,64
Boeing 777-200	54922	17623	6019	12038	12964	229517	190508	305	1851,177	2128,789	12936,24	1,493087	-4,9E-05	42,59
Boeing 777-200ER	58966	24947	10742	16298	17779	263083	195044	375	1460,41	2526,52	17753,69	1,52051	-5,3E-05	38,54
Boeing 777-300ER	51709	20416	10533	14585	15742	351535	237682	339	1894,443	3828,486	15721,31	3,050896	-0,00012	66,00
Boeing 787-8	43091	9074	10186	17536	18520	227930	161025	242	1874,491	4801,498	18511,83	2,392547	-8,2E-05	57,02
Boeing 787-9	54431	25310	9714	15223	17400	254692	181436	290	1637,484	4145,078	17393,39	2,510224	-0,00011	55,36
Boeing MD-80	17600	12701	2621	4389	5556	63503	50802	139	965,0002	2218,504	5544,298	2,048427	-0,00032	41,31
Bombardier CRJ100	5480	3800	1019	2593	3195	21523	19142	50	1293,047	577,8979	3097,539	-0,4218	0,000835	30,83
Bombardier CRJ200	5443	3629	1019	2685	3241	21523	19142	50	1248,388	744,3726	3182,951	-0,33353	0,000751	31,01
Bombardier CRJ700	8505	4536	1759	4260	5000	32999	28259	70	1234,317	2040,422	4989,462	1,640782	-0,00017	41,86
Bombardier CRJ900	9979	6940	1926	3630	4593	38329	31751	86	1019,615	2144,883	4573,839	1,942315	-0,00034	42,16
Bombardier CRJ1000	11975	9639	1815	3593	4649	41640	35153	104	861,3828	1615,143	4638,832	1,818908	-0,00037	35,18
De Havilland Canada Dash 8 Q100	3813	2750	926	1991	2519	15650	14061	37	1061,403	1460,066	2501,475	2,21639	-0,00054	53,60
De Havilland Canada Dash 8 Q300	6223	5289	715	1700	2130	19500	17920	50	823,8529	370,4924	2067,224	2,319608	-0,00058	39,77
De Havilland Canada Dash 8 Q400	8500	6468	1396	2847	3415	29257	25855	82	827,8432	962,1644	3393,53	1,953647	-0,00039	36,49
De Havilland Canada Twin Otter	1972	1124	610	1300	1413	5670	5349	19	1091,887	64244,65	3197,72	-20,9058	-0,00518	Out of range
Embraer E170	9400	5800	1945	4074	4954	35990	29600	78	1047,051	2234,342	4936,771	2,113435	-0,0003	45,22
Embraer E175	10200	6600	1815	3852	4705	37500	31700	84	1037,079	1959,115	4696,796	1,731812	-0,00027	39,38
Embraer E190	12900	6800	1801	4769	5602	47790	40800	106	1120,192	2110,568	5590,399	1,433197	-0,0001	38,14
Embraer E195	13800	7000	1482	4630	5463	48790	42500	118	1111,778	1740,064	5426,317	0,788318	0,000115	32,17
Embraer E195-E2	16100	12000	3519	5649	6927	61500	51850	146	968,6468	1758,619	6921,63	1,277012	-0,00017	29,94
Embraer EMB-120 Brasilia	3281	1700	537	2926	3287	11500	10500	30	-16,72	127,2083	3134,362	1,135023	0,000955	39,51
Embraer ERJ-145	5250	4600	1759	2222	3111	20600	17100	50	909,2933	2221,463	3118,857	1,835896	-0,00081	39,08
Fokker 100	10700	8400	2037	3111	3797	44450	36740	97	1023,47	1242,123	3752,454	2,528295	-0,00052	44,84
Saab 340	11454	10141	806	2248	2300	12700	11660	34	1088,193	-2,11257	3797	-0,07145	0,001058	33,61
Sukhoi Superjet 100	12245	6000	1722	5204	5723	45880	40000	98	1327,105	902,0608	5682,453	1,330804	3,86E-05	37,34

Figure 6.9 Fuel per Passenger Calculator

7 Summary and Conclusions

This thesis examined the fuel consumption of passenger aircraft using the bathtub curve, with the aim of simplifying fuel efficiency analysis across different aircraft and flight distances. The bathtub curve, which plots fuel consumption per passenger per 100 kilometers against range, was calculated for 50 of the most used commercial aircraft. Unlike traditional cruise-only methods, this approach included all flight phases, offering a more realistic assessment of fuel use.

To make the process more practical, a simplified analytical version of the bathtub curve was developed using five parameters. These were optimized in Excel and shown to closely match results from the full model. This analytical form allows for fast estimations and was implemented in Excel tools designed to help users quickly evaluate fuel use and select appropriate aircraft for given flight distances.

The thesis also extended the bathtub curve application to estimate absolute fuel consumption and investigated Intermediate Stop Operations (ISO) through a case study on the Perth–London route. The findings showed that splitting the route into two legs with an aircraft optimized for the flight distance could reduce fuel consumption per passenger. However, this benefit is not guaranteed. ISO introduces extra complexity, including additional fees, longer travel times, and potential inconvenience for passengers, which may outweigh the fuel savings.

In conclusion, the bathtub curve offers a powerful and accessible way to analyze aircraft fuel efficiency. The simplified model and developed tools provide valuable support for planning and environmental assessment. ISO, while promising in some scenarios, requires careful evaluation of operational trade-offs before implementation.

8 Recommendations

Based on the analysis of the bathtub curve for 50 of the most used passenger aircraft, the development of a simplified analytical model, and the evaluation of Intermediate Stop Operations (ISO), the following recommendations are proposed for future:

Expand the aircraft database: This project focused on the 50 most frequently operated passenger aircraft, with the majority being large commercial jetliners. While some regional jets, turboprops, and business aircraft were included, they represented only a small portion of the sample. Future work should expand the bathtub curve calculation to cover a wider variety of aircraft types, particularly to enable the study of the viability and sustainability of short-haul flights – an aspect increasingly questioned by policymakers in Europe.

Incorporate real operational data: Validate the analytical equation using actual fuel burn data from flight tracking and airline records, enabling a more realistic comparison with theoretical estimates. If airlines made such information publicly available, it would allow for a comparison between measured and calculated values.

Holistic ISO assessment: Future studies should integrate direct operating costs, passenger time value, airport slot availability, and climate impact models to produce a comprehensive cost–benefit framework for ISO. This assessment should also include the acquisition cost of the aircraft, since implementing ISO with a different aircraft type could potentially reduce capital expenditure compared to operating a single long-range aircraft for the entire route. In the present study, only the amount of fuel consumed was evaluated, without considering that the fuel price at the intermediate stop may be lower – as is often the case in some Middle Eastern countries– which could further improve the economic viability of ISO in certain scenarios.

List of References

AGARD, 1980. *Multilingual Aeronautical Dictionary*. Neuilly, France: Advisory Group for Aerospace Research and Development (AGARD/NATO).
Available from: http://MAD.Profscholz.de
Archived at: https://bit.ly/AGARD-1980.

AIRBUS, 2025. *Aircraft Characteristics – Airport and Maintenance Planning.* Toulouse, France: Airbus S.A.S.
Available from: http://bit.ly/AirbusAircraftCharacteristics
Archived at: https://perma.cc/QR2X-5YTX

ATANASOV, Georgi, VAN WENSVEEN, Jasper, PETER, Fabian, ZILL, Thomas, 2022. *Electric Commuter Transport Concept Enabled by Combustion Engine Range Extender.* Darmstadt, Germany: Deutscher Luft- und Raumfahrtkongress 2019.
Available from: https://doi.org/10.25967/490245

ATMOSFAIR, 2008. *Der Emissionsrechner*. Berlin, Germany: Atmosfair GmbH.
Available from: http://bit.ly/3HuglM2
Archived at: https://perma.cc/8FKA-85VA

AVIATION BROKER, 2025a. *ATR 42-500 Specifications*. Frankfurt, Germany: Aviation Broker.
Available from: https://bit.ly/ATR42specs
Archived at: https://perma.cc/PG9A-GKX9

AVIATION BROKER, 2025b. *ATR 72-500 Specifications*. Frankfurt, Germany: Aviation Broker.
Available from: https://bit.ly/ATR72specs
Archived at: https://perma.cc/Z5Q5-BBY5

AVIATION STRATEGY, 2019. *Icelandic Hubbing: Can Icelandair Live With Wow?*. In: Aviation Strategy, no. 228, pp. 10-14. London, UK: Aviation Strategy Ltd.
Available from: http://bit.ly/3Jep9WS
Archived at: https://perma.cc/U3UT-V7MC

BOEING, 2025. *Airplane Characteristics for Airport Planning*. Seal Beach, California, USA: Boeing Commercial Airplanes.
Available from: https://www.boeing.com/commercial/airports/plan-manuals
Archived at: https://perma.cc/L3F9-PXWP

BOMBARDIER, 2025a. *Airport Planning Manual Series 100/200/440.* Toronto, Ontario, Canada: Bombardier Inc.
Available from: https://bit.ly/BombardierSeries100APM
Archived at: https://perma.cc/SP4S-K6XL

BOMBARDIER, 2025b. *Airport Planning Manual Series 700.* Toronto, Ontario, Canada: Bombardier Inc.
Available from: https://bit.ly/BombardierSeries700
Archived at: https://perma.cc/C9H4-RVLT

BOMBARDIER, 2025c. *Airport Planning Manual Series 705/900.* Toronto, Ontario, Canada: Bombardier Inc.
Available from: https://bit.ly/BombardierSeries900
Archived at: https://perma.cc/63EA-4L8X

BOMBARDIER, 2025d. *Airport Planning Manual Series 1000.* Toronto, Ontario, Canada: Bombardier Inc.
Available from: https://bit.ly/BombardierSeries100
Archived at: https://perma.cc/U36R-FYBU

BURZLAFF, Marcus, 2017a. *Aircraft Fuel Consumption – Estimation and Visualization*. Project. Hamburg, Germany: Hamburg University of Applied Sciences.
Available from: http://nbn-resolving.org/urn:nbn:de:gbv:18302-aero2017-12-13.019

BURZLAFF, Marcus, 2017b. *Aircraft Fuel Consumption – Estimation and Visualization*. Dataset. Harvard Dataverse, V2.
Available from: https://doi.org/10.7910/DVN/2HMEHB

COLLINS, 2025. Fuel Consumption. In: *Collins English dictionary*.
Available from: https://www.collinsdictionary.com/dictionary/english/fuel-consumption

CROCKER, David, COLLIN, Peter, 2005. *Dictionary of Aviation*.
Available from: https://bit.ly/crocker-2005
Archived at: https://perma.cc/X9TG-DJKN

DE HAVILLAND, 2022. *Dash 8 Series Publications*. Downsview, Ontario, Canada: De Havilland Aircraft of Canada Limited.
Available from: https://dehavillandportal.com/airport-publications/arff#/
Archived at: https://perma.cc/DY6Q-7NCH

EGELHOFER, Regina, MARIZY, Corinne, BICKERSTAFF, Christine, 2008. *On How to Consider Climate Change in Aircraft Design*. In: Meteorologische Zeitschrift, vol. 17, no. 2, pp. 173-179. Stuttgart, Germany: Gebrüder Borntraeger.
Available from: https://doi.org/10.1127/0941-2948/2008/0281

ELLIS, Darren, 2019. *The Strategic Context of the Three Major Gulf Carriers*. In: Transportation research Procedia, no. 43, pp. 188-198. Cranfield, UK: Cranfield University.
Available from: https://doi.org/10.1016/j.trpro.2019.12.033

EMBRAER, 2025. *Airport and Firefighting Manuals - Airport Planning*. Putim, Brazil: Embraer S.A.
Available from: https://flyembraer.com
Archived at: https://perma.cc/LD5Z-3M6J

FILIPPONE, Antonio, 2012. *Advanced Aircraft Flight Performance*. Cambridge, UK: Cambridge University Press. p. 454. ISBN 978-1-139-78966-0.
Available from: https://bit.ly/advanced_aircraft_flight_performance

FLIGHTAWARE, 2025. *QFA9 Flight Track: Perth (YPPH) to London Heathrow (EGLL), July 2, 2025*. Live Flight Tracking. Houston, Texas, USA: FlightAware.
Available from: http://bit.ly/flightawareQFA9
Archived at: https://perma.cc/9D8T-FWSV

FOKKER, 2025. *Information Booklet Fokker 100*. Hoofddorp, Netherlands: Fokker Services Group.
Available from: https://fokkerservicesgroup.com/media/emccsdnm/fsg_fokker-100.pdf
Archived at: https://perma.cc/UB9U-EH6X

HARPER COLLINS PUBLISHERS, 2025. Fuel Consumption. In: *Collins Dictionary*.
Available from: https://www.collinsdictionary.com/dictionary/english/fuel-consumption

HARTJES, Sander, BOS, Frank, 2015. *Evaluation of Intermediate Stop Operations in Long-Haul Flights*. Delft, Netherlands: Delft University of Technology.
Available from: https://doi.org/10.1016/j.trpro.2015.09.049

HIRSCH, Sebastian, 2022. *The 50 Most Important Parameters of the 60 Most Used Passenger Aircraft*. Project. Hamburg, Germany: Hamburg University of Applied Sciences.
Available from: https://nbn-resolving.org/urn:nbn:de:gbv:18302-aero2022-10-01.013

HIRSCH, Sebastian, 2024. *The 50 Most Important Parameters of the 60 Most Used Passenger Aircraft*. Dataset. Harvard Dataverse, V2.
Available from: https://doi.org/10.7910/DVN/YAHODP

ICAO, 2025. *Freedoms of the Air.* Montréal, Québec, Canada: International Civil Aviation Organization (ICAO).
Available from: https://www.icao.int/pages/freedomsair.aspx
Archived at: https://perma.cc/YM7B-SYXU

KÜHN, Marius, 2023. *Fuel Consumption of the 50 Most Used Passenger Aircraft.* Project. Hamburg, Germany: Hamburg University of Applied Sciences.
Available from: https://purl.org/aero/POS2023-09-19b
Open Access at: https://doi.org/10.48441/4427.1045

KÜHN, Marius, 2024. *Fuel Consumption of the 50 Most Used Passenger Aircraft.* Dataset. Harvard Dataverse, V3.
Available from: https://doi.org/10.7910/DVN/4CYNKA

LINKE, Florian, GREWE, Volker, GOLLNICK, Volker, 2016. *The Implications of Intermediate Stop Operations on Aviation Emissions and Climate.* In: Meteorologische Zeitschrift Vol. 26 No. 6 (2017), pp. 697 - 709. Hamburg, Germany: Deutsches Zentrum für Luft- und Raumfahrt, Einrichtung Lufttransportsysteme.
Available from: https://doi.org/10.1127/metz/2017/0763

MYCLIMATE, 2025. *Flight Emission Calculator.* Zürich, Switzerland: Foundation Myclimate.
Available from: https://bit.ly/myclimate_emission
Archived at: https://perma.cc/4KVF-TFNY

PARAMOUNT BUSINESS JETS, 2025. Leg. In: *Glossary of Aviation Terms*.
Available from: https://www.paramountbusinessjets.com/aviation-terminology/leg
Archived at: https://perma.cc/R8MJ-F8YJ

PARAMOUNT BUSINESS JETS, 2025. Stage Length. In: *Glossary of Aviation Terms*.
Available from: https://bit.ly/3H83krr
Archived at: https://perma.cc/GKK7-PKGF

RAYTHEON, 2025. *Beechcraft 1900D Passenger Specifications and Performance*. Arlington, Virginia, USA: RTX.
Archived at: https://perma.cc/8SK8-UU2G

RÖSING, Christian, 2021. *Analysis of Flight Routes and Hints for Passengers.* Project. Hamburg, Germany: Hamburg University of Applied Sciences.
Available from: https://www.fzt.haw-hamburg.de/pers/Scholz/arbeiten/TextRoesing.pdf

SAAB, 2005. *Saab 340 Airplane Characteristics for Airport Planning*. Linköping, Sweden: Saab Aircraft AB.
Available from: https://bit.ly/Saab340AirportPlanning
Archived at: https://perma.cc/8Y8S-2AMW

SCHOLZ, Dieter, 2015. *Aircraft Design*. Lecture Notes. Hamburg, Germany: Hamburg University of Applied Sciences.
Available from: http://LectureNotes.AircraftDesign.org

SCHOLZ, Dieter, 2025. *Ecolabel for Aircraft*. Hamburg, Germany: Hamburg University of Applied Sciences.
Available from: http://Ecolabel.ProfScholz.de

THOR, Robin N., NIKLAß, Malte, DAHLMANN, Katrin, LINKE, Florian, GREWE, Volker, MATTHES, Sigrun, 2023. *The CO2 and non-CO2 climate effects of individual flights: simplified estimation of CO2 equivalent emission factors*. In: Geoscientific Model Development Discussions. Göttingen, Germany: Copernicus Gesellschaft mbH.
Retracted from: https://gmd.copernicus.org/preprints/gmd-2023-126/
Available at: https://bit.ly/ClimateEffectsFlights

TORENBEEK, Egbert, 1976. *Synthesis of Subsonic Airplane Design: An Introduction to the Preliminary Design of Subsonic General Aviation and Transport Aircraft, with Emphasis on Layout, Aerodynamic Design, Propulsion, and Performance.* Delft, Netherlands: Delft University Press.
Available from: https://dx.doi.org/10.1007/978-94-017-3202-4
Open Access at: https://bit.ly/4m19j0g

UNITED NATIONS, 2025. *International Air Services Transit Agreement*. New York, USA: United Nations Treaty Collection.
Available from: https://treaties.un.org/Pages/showDetails.aspx?objid=0800000280156f42
Archived at: https://perma.cc/5Y7X-UJB5

VIKING AIR, 2025a. *Twin Otter Series 400 Brochure*. North Saanich, British Columbia, Canada: Viking Air Limited.
Available from: http://bit.ly/40EdR4h
Archived at: https://perma.cc/Y4RQ-S45U

VIKING AIR, 2025b. *Twin Otter Series 400 Technical Specifications & Standard Equipment List*. North Saanich, British Columbia, Canada: Viking Air Limited.
Available from: http://bit.ly/41dNgv3
Archived at: https://perma.cc/2TNN-76UP

WIKIDOT, 2012. *Sukhoi Superjet 100 – Payload Range*. Toruń, Poland: Wikidot.
Available from: http://superjet.wikidot.com/wiki:payload-range
Archived at: https://perma.cc/5S3M-9W2K

WIKIPEDIA, 2025a. Example Values: Fuel economy in aircraft. In *Wikipedia, The Free Encyclopedia*.
Available from: https://bit.ly/wikipedia_Example_Values
Archived at: https://perma.cc/6MPD-JK7J

WIKIPEDIA, 2025b. Fuel economy in aircraft. In *Wikipedia, The Free Encyclopedia*.
Available from: https://bit.ly/wikipedia_Flight_Distance
Archived at: https://perma.cc/6MPD-JK7J

ZENGERLING, Zarah Lea, LINKE, Florian, WEDER, Christian Martin, DAHLMANN, Katrin, 2022. *Climate-Optimised Intermediate Stop Operations: Mitigation Potential and Differences from Fuel-Optimised Configuration*. In: Applied Sciences 12, no. 23: 12499.
Available from: https://doi.org/10.3390/app122312499

All online resources have been accessed on 2025-07-11 or later.

Appendix A Bathtub Curves of the Most Used Passenger Aircraft

Airbus A220-300

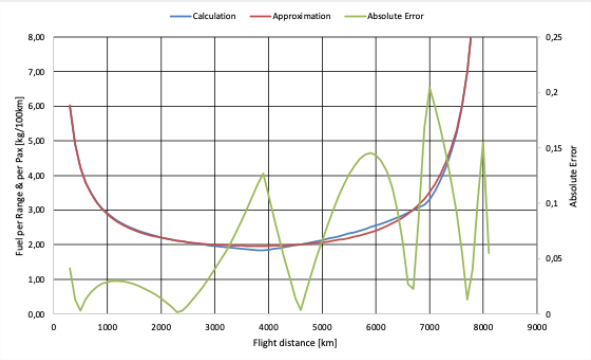

Airbus A319

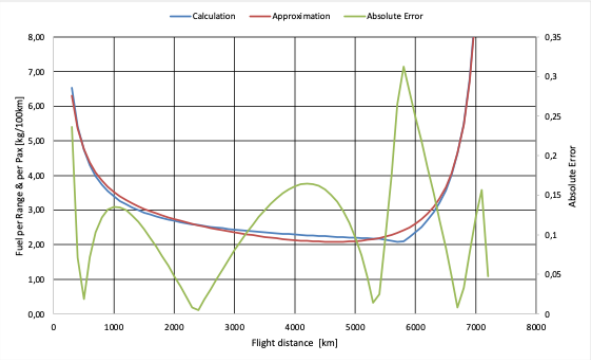

Airbus A320

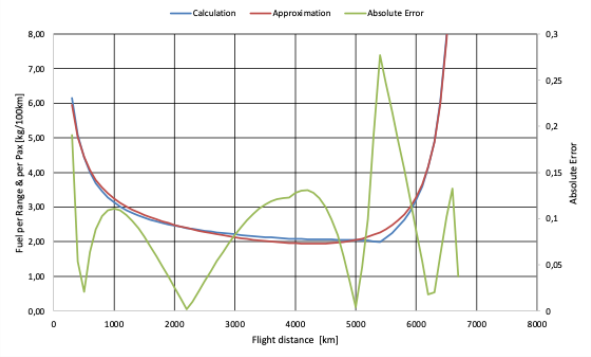

Airbus A320neo

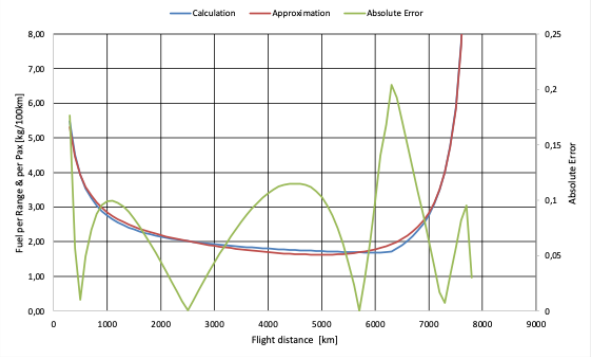

Airbus A321

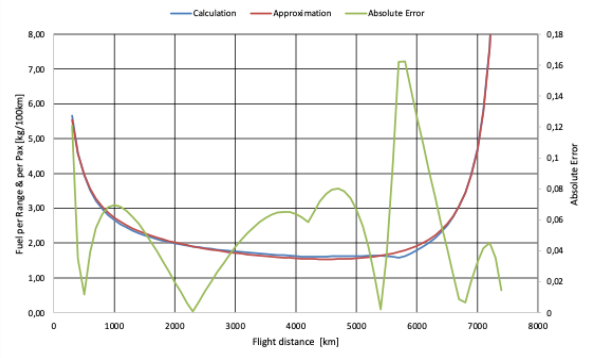

Airbus A321neo

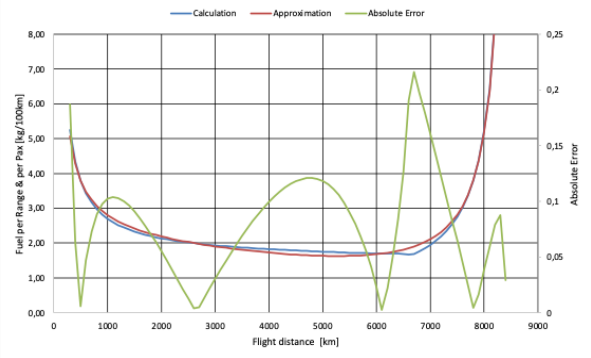

Airbus A330-200

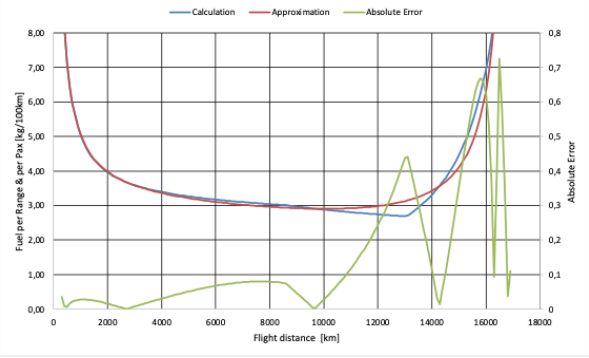

Airbus A330-300

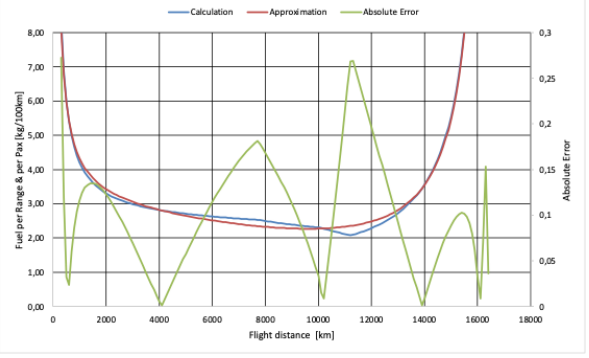

Airbus A330-900

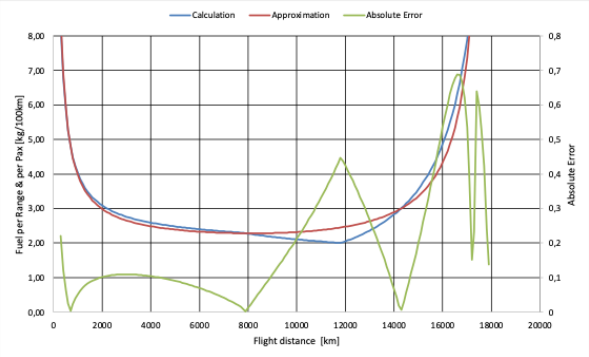

Airbus A350-900

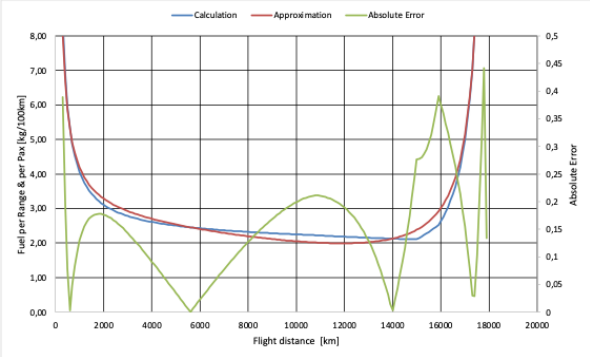

Airbus A380-800

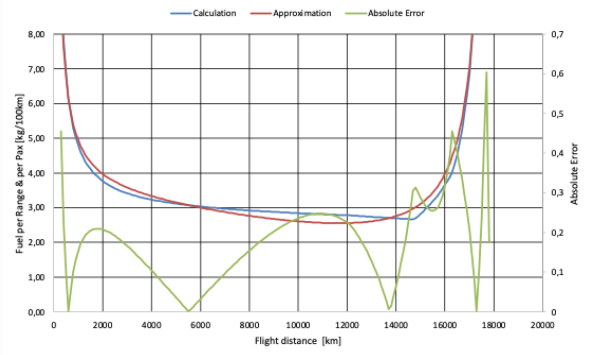

ATR 42

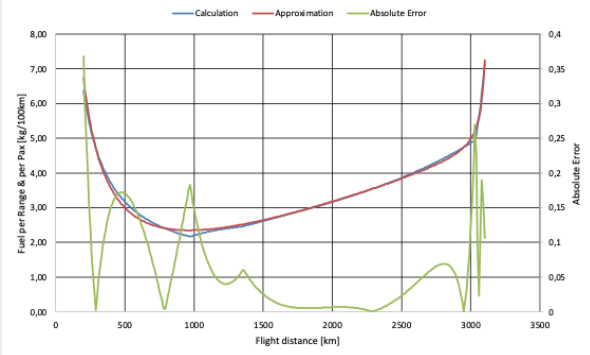

ATR 72

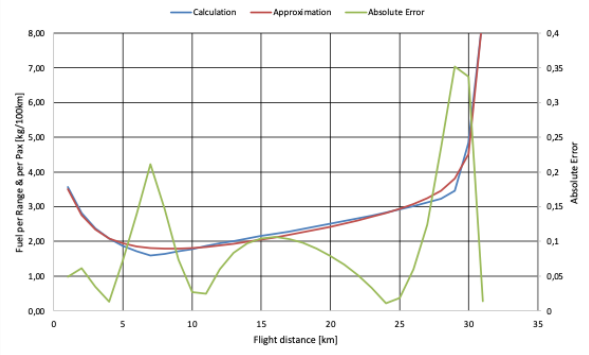

Beechcraft 1900D

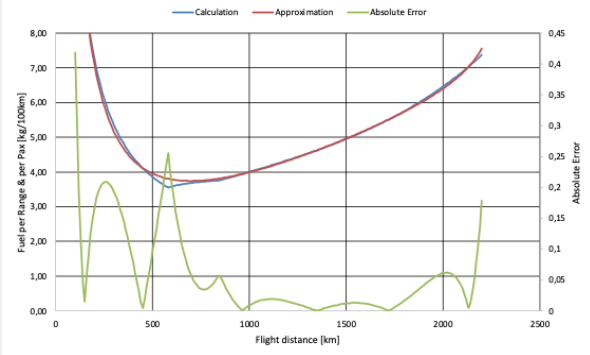

Boeing 717-200

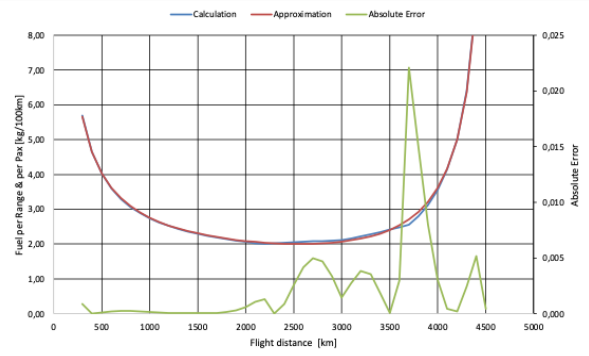

Boeing 737 Max 8

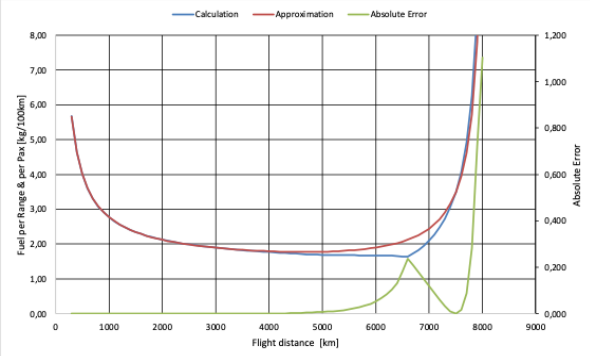

Boeing 737 MAX 9

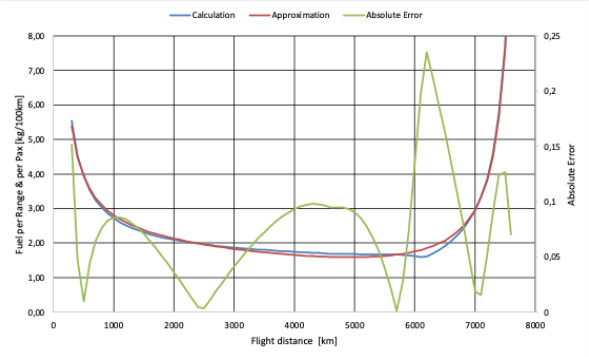

Boeing 737-300

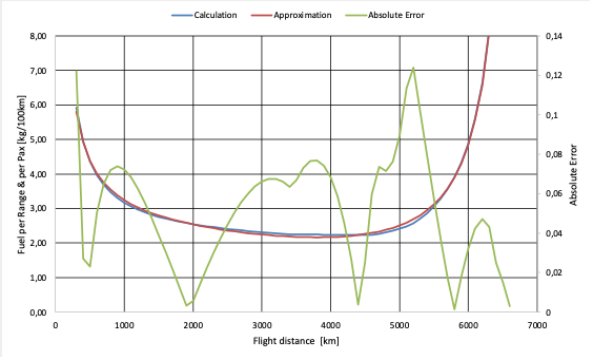

Boeing 737-400

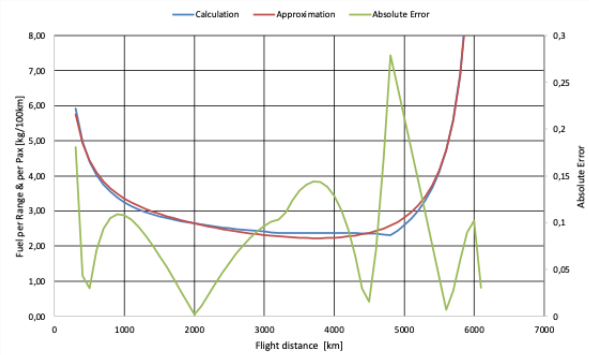

Boeing 737-500

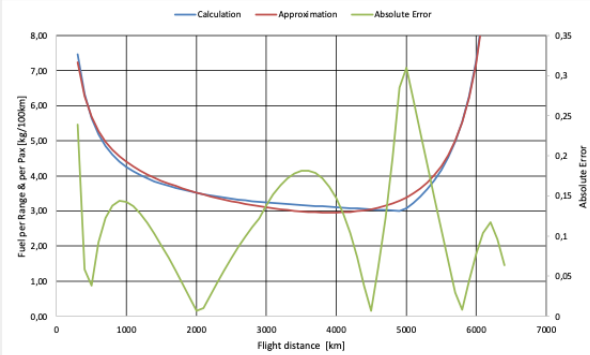

Boeing 737-700

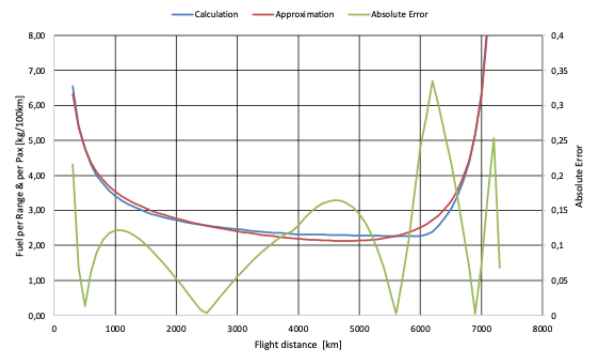

Boeing 737-800

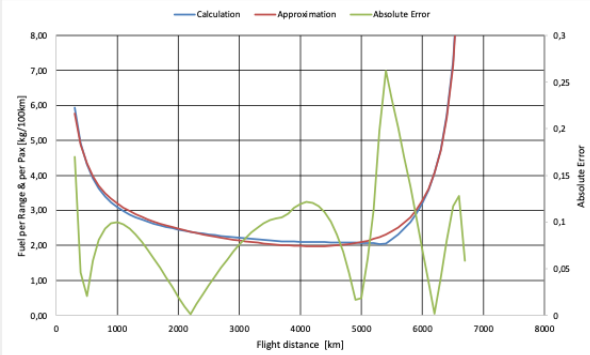

Boeing 737-900

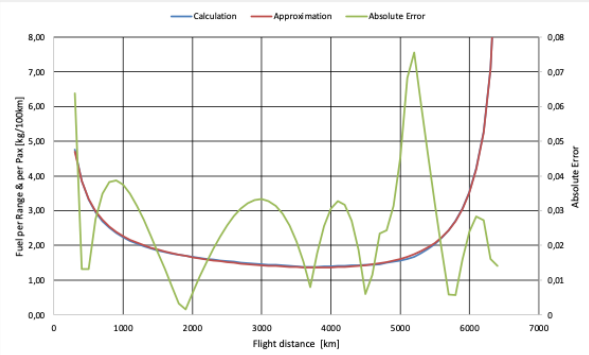

Boeing 747-400

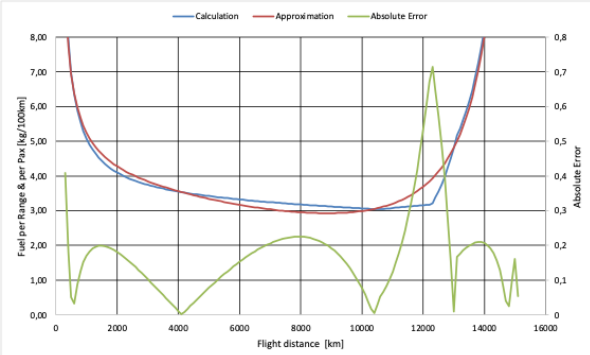

Boeing 757-200

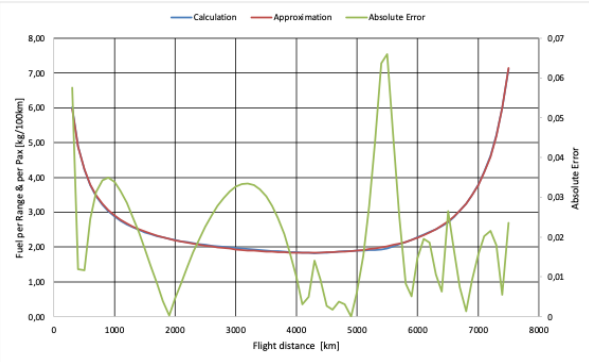

Boeing 767-300

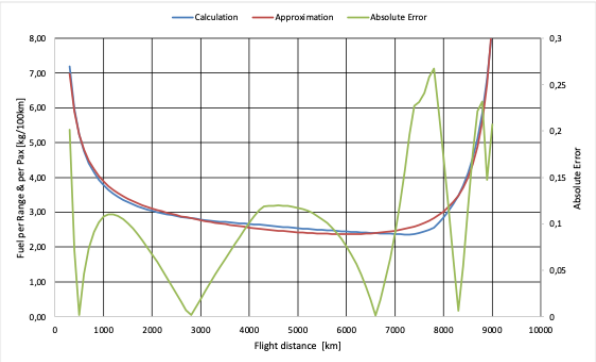

Boeing 777-200

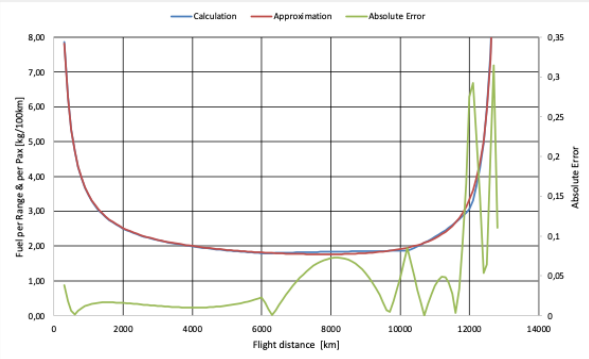

Boeing 777-200ER

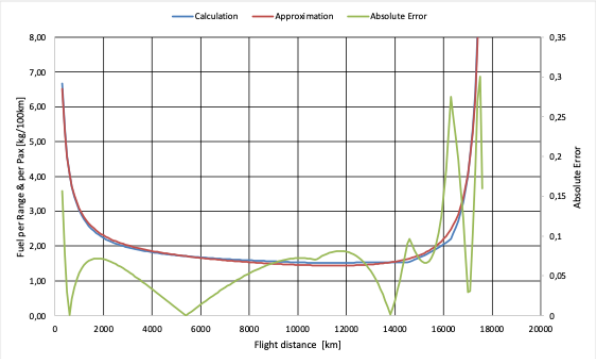

Boeing 777-300ER

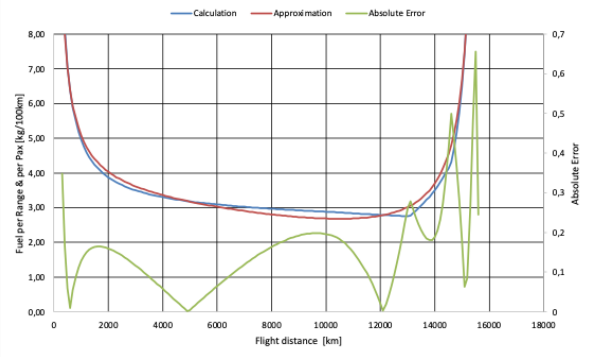

Boeing 787-8

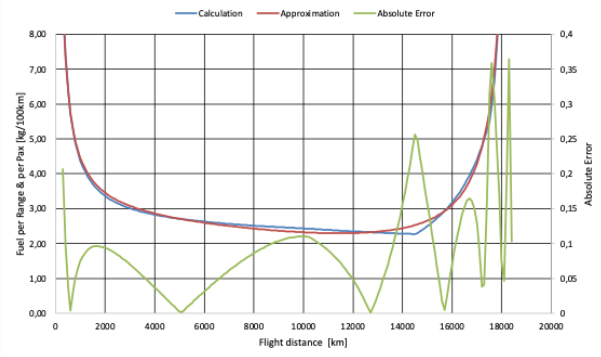

Boeing 787-9

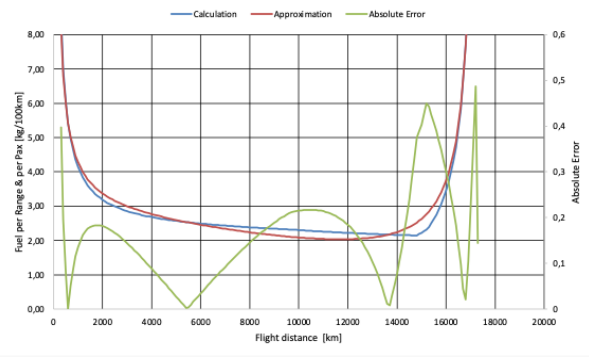

Boeing MD-80

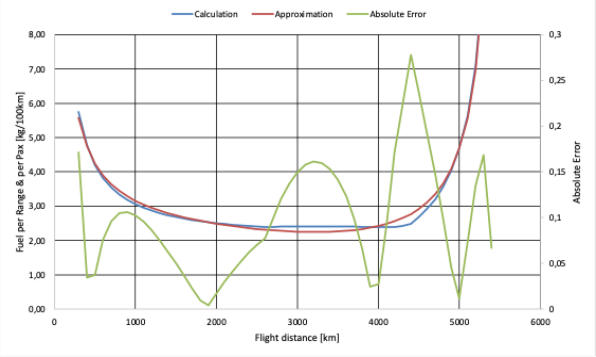

Bombardier CRJ100

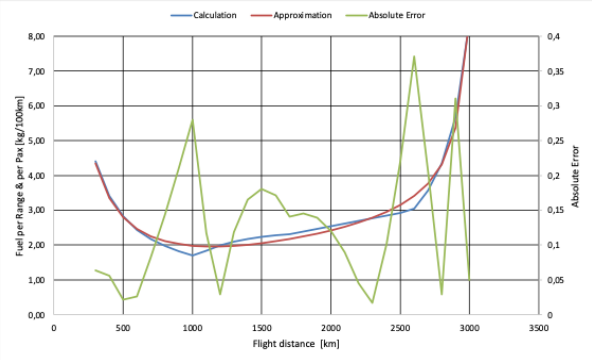

Bombardier CRJ200

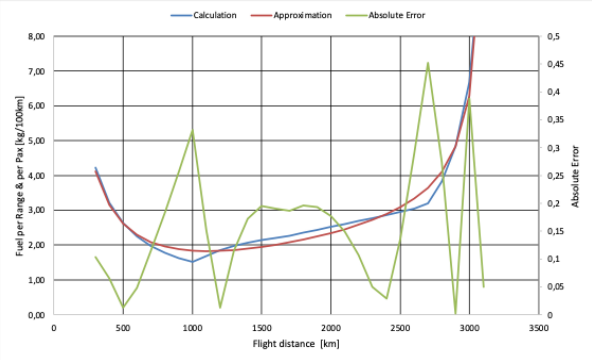

Bombardier CRJ700

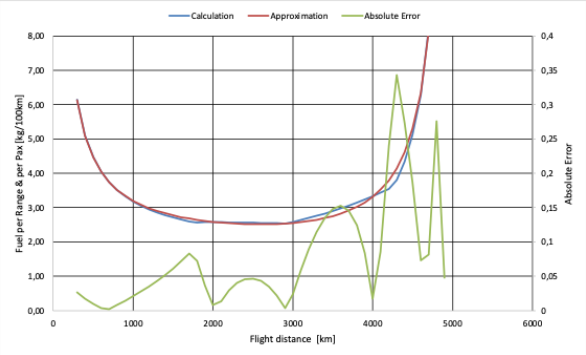

Bombardier CRJ900

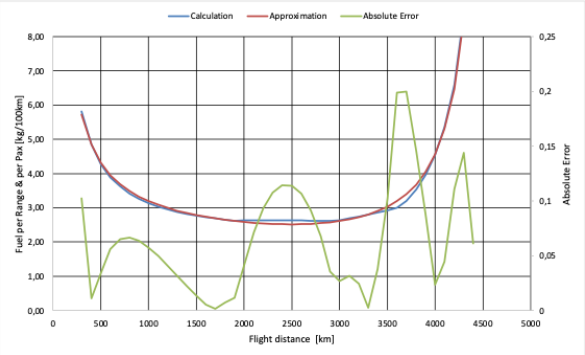

Bombardier CRJ1000

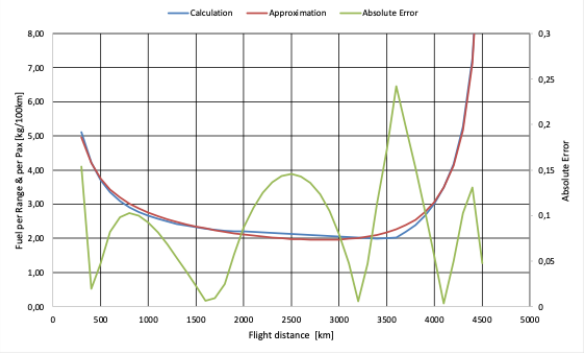

De Havilland Canada Dash 8 Q100

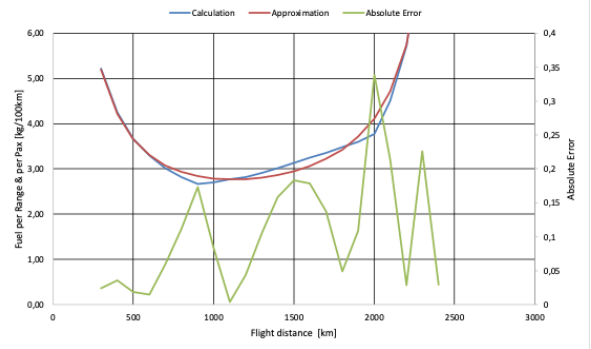

De Havilland Canada Dash 8 Q300

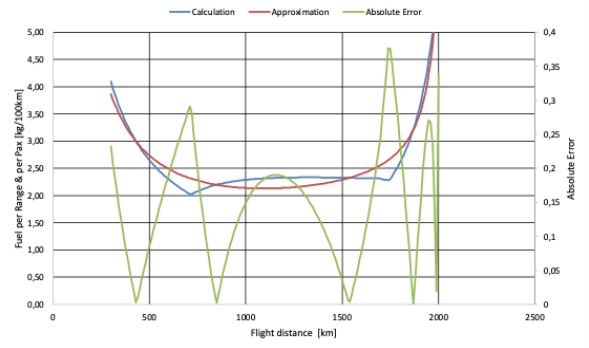

De Havilland Canada Dash 8 Q400

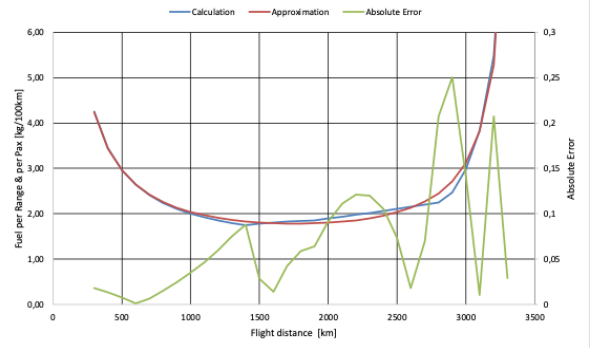

De Havilland Canada Twin Otter

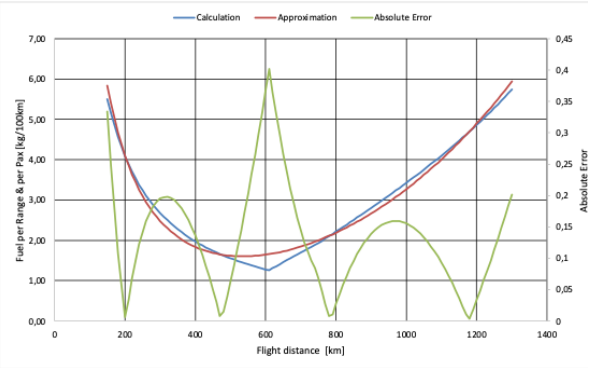

Embraer E170

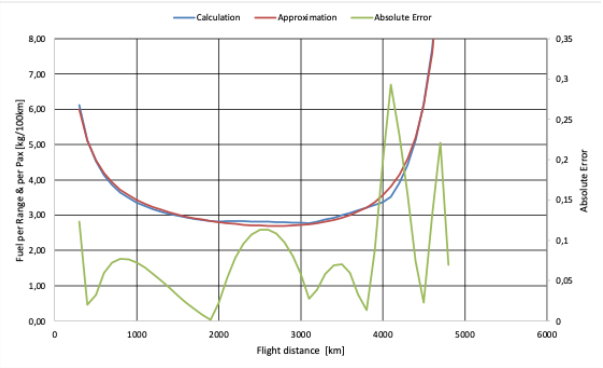

Embraer E175

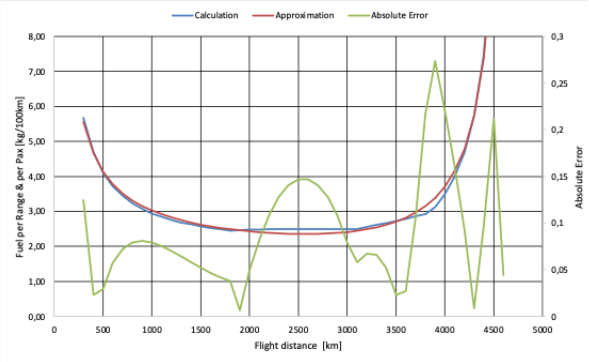

Embraer E190

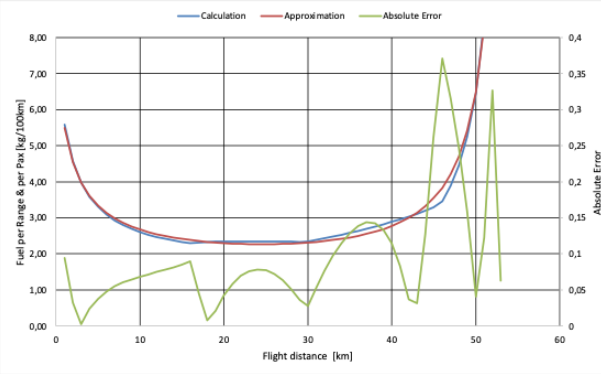

Embraer E195

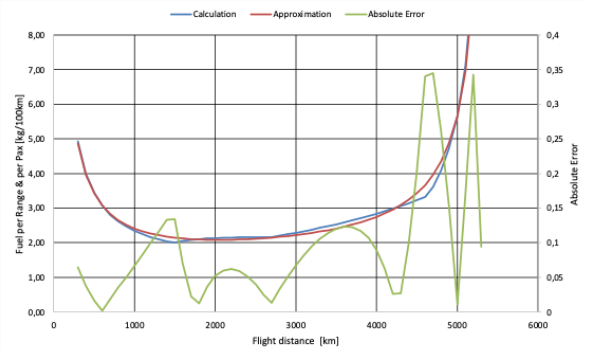

Embraer E195-E2

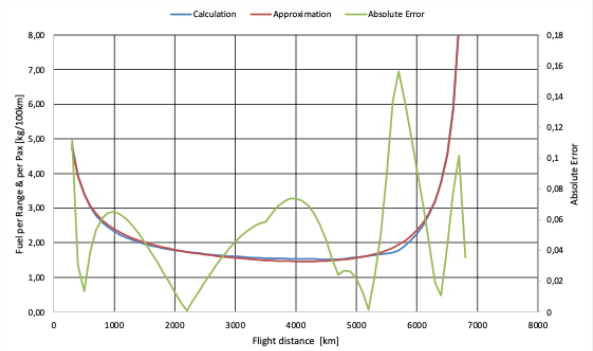

Embraer EMB-120 Brasilia

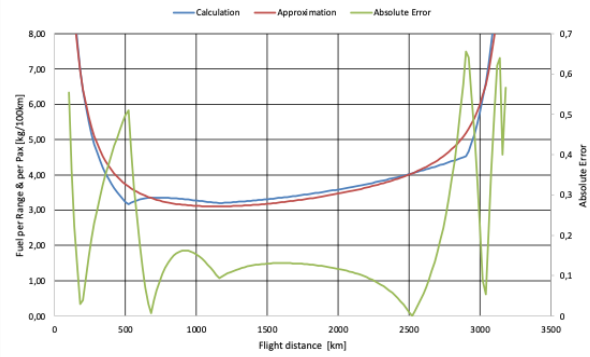

Embraer ERJ-145

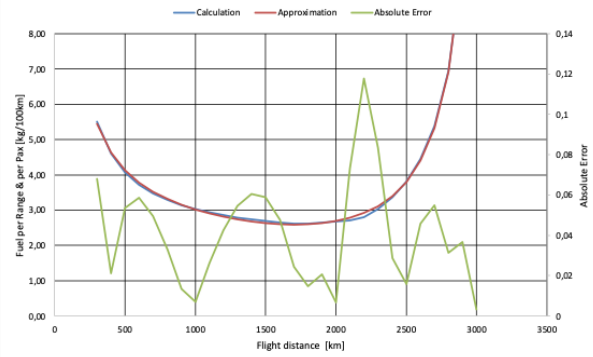

Fokker 100

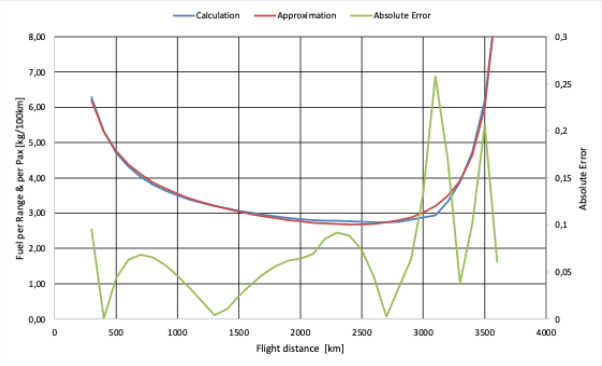

Saab 340

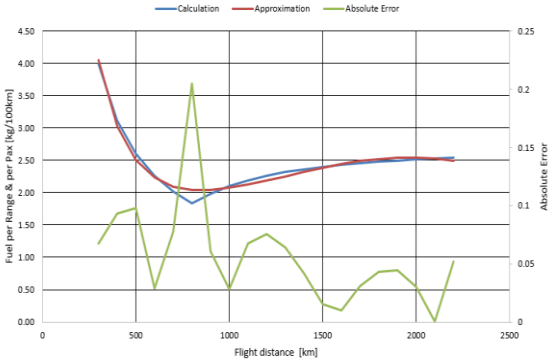

Sukhoi Superjet 100

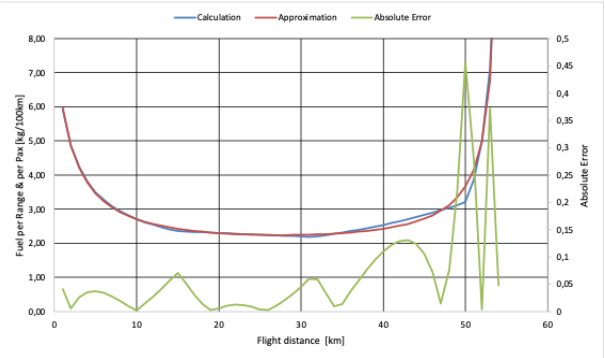

Appendix B Parameters for the Analytical Bathtub Curve

Aircraft Type	*a* *kg·km/(100 km)*	*b* *kg·km/(100 km)*	*c* *km*	*d* *kg/(100 km)*	*e* *kg/(100 km²)*
Airbus A220-300	1348,12031	3337,49771	8233,76489	1,13754164	-7,419E-05
Airbus A319	1113,75406	2519,36874	7297,19973	2,32059919	-0,0003073
Airbus A320	1089,05003	2243,80354	6797,39028	2,0668814	-0,0002967
Airbus A320neo	999,196298	2219,55227	7898,35527	1,74686869	-0,0002174
Airbus A321	1156,73696	2235,46156	7500,23147	1,42895945	-0,0001986
Airbus A321neo	920,134195	2444,50705	8498,74378	1,75714258	-0,0002013
Airbus A330-200	2062,14959	4583,80728	16995,1223	2,79213931	-7,467E-05
Airbus A330-300	1571,74585	7785,79738	16501,8393	2,40711845	-0,0001496
Airbus A330-900	1945,75286	6123,7285	17999,2765	1,69701712	-3,429E-05
Airbus A350-900	1629,38613	4438,50048	17994,373	2,40891967	-0,0001076
Airbus A380-800	1726,00705	5481,70846	17893,6254	3,02129494	-0,0001284
ATR 42	1398,63148	78,2265422	3128,55446	-0,6093329	0,00150163
ATR 72	1021,19546	213,726646	3339,14969	-0,1621599	0,00089199
Beechcraft 1900D	1307,759	230,607723	2377,1471	-0,0952914	0,00261495
Boeing 717-200	1196,82939	1957,9112	4626,6299	1,32893563	-0,0002819
Boeing 737 Max 8	1225,96207	1539,86988	8125,80198	1,40208079	-7,204E-05
Boeing 737 MAX 9	1059,14494	1931,27533	7766,19224	1,65600107	-0,0001953
Boeing 737-300	1032,5886	3189,81182	6701,81861	1,95602518	-0,0003054
Boeing 737-400	938,482348	2594,42211	6198,83284	2,28615404	-0,0003651
Boeing 737-500	1105,15914	3838,04122	6567,75043	3,07735743	-0,0004725
Boeing 737-700	1127,71942	2286,30903	7400,53333	2,32996192	-0,0002736
Boeing 737-800	1036,45963	2331,88753	6843,21636	2,04216562	-0,0002843
Boeing 737-900	1003,04287	1924,90615	6576,11682	1,10233456	-0,0001823
Boeing 747-400	1594,23834	10245,1615	15286,4124	3,16611086	-0,000227
Boeing 757-200	1278,78053	3347,9712	7990,00222	1,30863998	-0,0001565
Boeing 767-300	1285,86447	2254,16349	9305,30218	2,497284	-0,0001703
Boeing 777-200	1851,17737	2128,78859	12936,2415	1,49308696	-4,923E-05
Boeing 777-200ER	1460,41002	2526,51959	17753,6895	1,52050981	-5,337E-05
Boeing 777-300ER	1894,4431	3828,48586	15721,3132	3,05089611	-0,0001223
Boeing 787-8	1874,49054	4801,49763	18511,826	2,39254684	-8,215E-05
Boeing 787-9	1637,48389	4145,07792	17393,3907	2,51022395	-0,0001148
Boeing MD-80	965,00016	2218,50361	5544,29755	2,04842731	-0,0003243
Bombardier CRJ100	1293,04681	577,897856	3097,53886	-0,4217952	0,00083543
Bombardier CRJ200	1248,38757	744,372575	3182,95081	-0,3335254	0,00075097
Bombardier CRJ700	1234,3174	2040,42222	4989,46155	1,64078241	-0,0001718
Bombardier CRJ900	1019,61466	2144,88252	4573,83851	1,9423153	-0,0003393
Bombardier CRJ1000	861,382773	1615,14271	4638,83176	1,81890804	-0,0003748
De Havilland Canada Dash 8 Q100	1250,2926	1159,81588	2492,54761	0,38421117	0,00037556

De Havilland Canada Dash 8 Q300	937,053595	226,133581	2050,81286	0,44833323	0,00053985
De Havilland Canada Dash 8 Q400	979,026448	792,650618	3388,23167	0,71416547	1,3991E-05
De Havilland Canada Twin Otter	1105,5714	66095,3876	3277,17454	-21,925989	-0,0049347
Embraer E170	1047,05092	2234,3416	4936,77106	2,11343541	-0,0002981
Embraer E175	1037,07948	1959,11517	4696,79609	1,73181169	-0,0002738
Embraer E190	1126,41372	2092,92469	5590,12366	1,36139478	-8,64E-05
Embraer E195	1111,77805	1740,06361	5426,31701	0,7883178	0,00011467
Embraer E195-E2	968,646786	1758,61945	6921,62967	1,2770117	-0,0001676
Embraer EMB-120 Brasilia	967,650845	604,593761	3235,11011	1,26764222	0,00061372
Embraer ERJ-145	909,293314	2221,46253	3118,85724	1,83589603	-0,000806
Fokker 100	1023,4705	1242,12295	3752,45404	2,52829542	-0,0005152
Saab 340	1088,19304	-2,112568	3797	-0,0714534	0,00105846
Sukhoi Superjet 100	1327,10508	902,060755	5682,45305	1,33080437	3,8611E-05

Aircraft Type	*Consumption RA (kg/100 km)*	*Mimimum Fuel Stage Length (km)*	*Mimimum Fuel (kg/100 km)*	*Delta Consumption (%)*
Airbus A220-300	1.964	3782	1.963	0.037%
Airbus A319	2.083	4648	2.083	0.002%
Airbus A320	1.965	4287	1.943	1.157%
Airbus A320neo	1.642	4965	1.626	1.003%
Airbus A321	1.547	4538	1.537	0.618%
Airbus A321neo	1.641	5270	1.628	0.779%
Airbus A330-200	2.936	10052	2.907	1.014%
Airbus A330-300	2.342	9661	2.263	3.509%
Airbus A330-900	2.280	8173	2.278	0.088%
Airbus A350-900	2.014	11891	1.993	1.058%
Airbus A380-800	2.558	11660	2.552	0.222%
ATR 42	2.325	960	2.325	0.006%
ATR 72	1.855	1046	1.840	0.807%
Beechcraft 1900D	5.791	696	3.741	
Boeing 717-200	2.063	2570	2.022	2.001%
Boeing 737 Max 8	1.775	4663	1.774	0.092%
Boeing 737 MAX 9	1.596	4923	1.589	0.464%
Boeing 737-300	2.184	3794	2.166	0.793%
Boeing 737-400	2.267	3748	2.227	1.804%
Boeing 737-500	3.131	3913	2.957	5.914%
Boeing 737-700	2.198	4743	2.130	3.179%
Boeing 737-800	2.006	4232	1.977	1.484%
Boeing 737-900	1.368	3809	1.367	0.086%
Boeing 747-400	3.090	8851	2.929	5.487%
Boeing 757-200	1.841	4174	1.839	0.094%
Boeing 767-300	2.520	5998	2.372	6.270%
Boeing 777-200	1.812	7773	1.761	2.908%
Boeing 777-200ER	1.443	11492	1.438	0.400%
Boeing 777-300ER	2.681	10483	2.681	0.003%
Boeing 787-8	2.317	11456	2.296	0.912%
Boeing 787-9	2.103	11678	2.035	3.360%
Boeing MD-80	2.325	3236	2.258	2.978%
Bombardier CRJ100	1.976	1145	1.960	0.838%
Bombardier CRJ200	2.001	1157	1.982	0.962%
Bombardier CRJ700	2.672	2593	2.523	5.911%
Bombardier CRJ900	2.628	2506	2.536	3.631%
Bombardier CRJ1000	2.185	2812	1.955	11.750%
De Havilland Canada Dash 8 Q100	2.823	1122	2.766	2.038%
De Havilland Canada Dash 8 Q300	2.314	1092	2.132	8.555%

De Havilland Canada Dash 8 Q400	1.833	1764	1.782	2.863%
De Havilland Canada Twin Otter	1.657	535	1.604	3.342%
Embraer E170	2.819	2690	2.695	4.585%
Embraer E175	2.486	2566	2.353	5.665%
Embraer E190	2.384	2666	2.269	5.035%
Embraer E195	2.150	2042	2.081	3.292%
Embraer E195-E2	1.479	4123	1.449	2.071%
Embraer EMB-120 Brasilia	3.673	1135	3.105	18.313%
Embraer ERJ-145	2.569	1709	2.566	0.098%
Fokker 100	2.705	2412	2.637	2.608%
Saab 340	2.131	1014	2.074	2.740%
Sukhoi Superjet 100	2.396	2914	2.225	7.694%
			average:	2.810%

Appendix C Aircraft Data Sources

Airbus A220-300	Airbus 2025; Hirsch 2024
Airbus A319	Airbus 2025; Hirsch 2024
Airbus A320	Airbus 2025; Hirsch 2024
Airbus A320neo	Airbus 2025; Hirsch 2024
Airbus A321	Airbus 2025; Hirsch 2024
Airbus A321neo	Airbus 2025; Hirsch 2024
Airbus A330-200	Airbus 2025; Hirsch 2024
Airbus A330-300	Airbus 2025; Hirsch 2024
Airbus A330-900	Airbus 2025; Hirsch 2024
Airbus A350-900	Airbus 2025; Hirsch 2024
Airbus A380-800	Airbus 2025; Hirsch 2024
ATR 42	Aviation Broker 2025a; Hirsch 2024
ATR 72	Aviation Broker 2025b; Hirsch 2024
Beechcraft 1900D	Raytheon 2025; Hirsch 2024; Atanasov 2022;
Boeing 717-200	Boeing 2025; Hirsch 2024
Boeing 737 Max 8	Boeing 2025
Boeing 737 MAX 9	Boeing 2025
Boeing 737-300	Boeing 2025; Hirsch 2024
Boeing 737-400	Boeing 2025; Hirsch 2024
Boeing 737-500	Boeing 2025; Hirsch 2024
Boeing 737-700	Boeing 2025; Hirsch 2024
Boeing 737-800	Boeing 2025; Hirsch 2024
Boeing 737-900	Boeing 2025; Hirsch 2024
Boeing 747-400	Boeing 2025; Hirsch 2024
Boeing 757-200	Boeing 2025; Hirsch 2024
Boeing 767-300	Boeing 2025; Hirsch 2024
Boeing 777-200	Boeing 2025; Hirsch 2024
Boeing 777-200ER	Boeing 2025; Hirsch 2024
Boeing 777-300ER	Boeing 2025; Hirsch 2024
Boeing 787-8	Boeing 2025; Hirsch 2024
Boeing 787-9	Boeing 2025; Hirsch 2024
Boeing MD-80	Boeing 2025; Hirsch 2024
Bombardier CRJ100	Bombardier 2025a
Bombardier CRJ200	Bombardier 2025a; Hirsch 2024
Bombardier CRJ700	Bombardier 2025b; Hirsch 2024
Bombardier CRJ900	Bombardier 2025c; Hirsch 2024
Bombardier CRJ1000	Bombardier 2025d
De Havilland Canada Dash 8 Q100	De Havilland 2022; Hirsch 2024
De Havilland Canada Dash 8 Q300	De Havilland 2022; Hirsch 2024
De Havilland Canada Dash 8 Q400	De Havilland 2022; Hirsch 2024

De Havilland Canada Twin Otter	Viking Air 2025a; Viking Air 2025b
Embraer E170	Embraer 2025; Hirsch 2024
Embraer E175	Embraer 2025; Hirsch 2024
Embraer E190	Embraer 2025; Hirsch 2024
Embraer E195	Embraer 2025; Hirsch 2024
Embraer E195-E2	Embraer 2025; Hirsch 2024
Embraer EMB-120 Brasilia	Embraer 2025; Hirsch 2024
Embraer ERJ-145	Embraer 2025; Hirsch 2024
Fokker 100	Fokker 2025; Hirsch 2024
Saab 340	Saab 2005; Hirsch 2024
Sukhoi Superjet 100	Wikidot 2025; Hirsch 2024